Spatial and temporal variations in depositional systems in the Kazusa Group: insights into the origins of deep-water massive sandstones in a Pleistocene forearc basin on the Boso Peninsula, Japan

Akihiko Takao[1], Keisuke Nakamura[2,6], Shinichi Takaoka[3], Masaya Fuse[4], Yohei Oda[5], Yasushi Shimano[6,8], Naohisa Nishida[7] and Makoto Ito[8*]

Abstract

A detailed chronostratigraphic framework established by the mapping of tephra key beds and application of oxygen isotopic data allows assessment of the synchroneity and diachroneity of depositional systems formed in coastal and deep-water environments. This framework also allows estimation of the timing of active delivery of coarse-grained sediments beyond the shelf margin in relation to relative sea-level changes. The depositional processes of deep-water massive sandstones (DWMSs) are still enigmatic; their formation is a result of active delivery of sands in association with the supply of organic carbon into deep-water environments. DWMSs are also important as reservoirs for hydrocarbon explorations. This study investigated the origins of DWMSs in the upper Umegase, Kokumoto, and Chonan formations (in ascending order) of the Pleistocene Kazusa Group on the Boso Peninsula, central Japan. Each formation contains several packets of DWMSs that are interpreted to have formed in response to the progradation of gravelly shelf-margin deltas or fan deltas during the falling and lowstand stages of relative sea-level changes controlled primarily by glacioeustasy. The development of DWMSs and associated sandstone beds is interpreted to have been induced by hyperpycnal flows, in association with sediment gravity flows that were initiated by breaching and/or collapse of sandy substrates on the shelf-margin deltas or fan deltas. The timings of the initial and final deposition of the packets vary within and between the formations, and are considered to have been controlled by the interaction between allogenic and autogenic processes operating in the gravelly shelf-margin deltas or fan deltas. A muddy horizon that contains the Lower–Middle Pleistocene Subseries boundary (the base of the Chibanian Stage) in the Kokumoto Formation is also underlain and overlain by the packets and represents a deposit formed in a condensed section in an upper slope environment. This depositional setting may have favored the development of the Global Boundary Stratotype Section and Point (GSSP) for the Lower–Middle Pleistocene Subseries boundary in the formation.

Keywords: Deep-water massive sandstones, Sediment gravity flows, Shelf-margin delta and fan delta, Slope apron, Hyperpycnal flow, Glacioeustasy, Falling and lowstand stages, Kazusa Group

* Correspondence: mito@faculty.chiba-u.jp
[8]Department of Earth Sciences, Chiba University, Chiba 263-8522, Japan
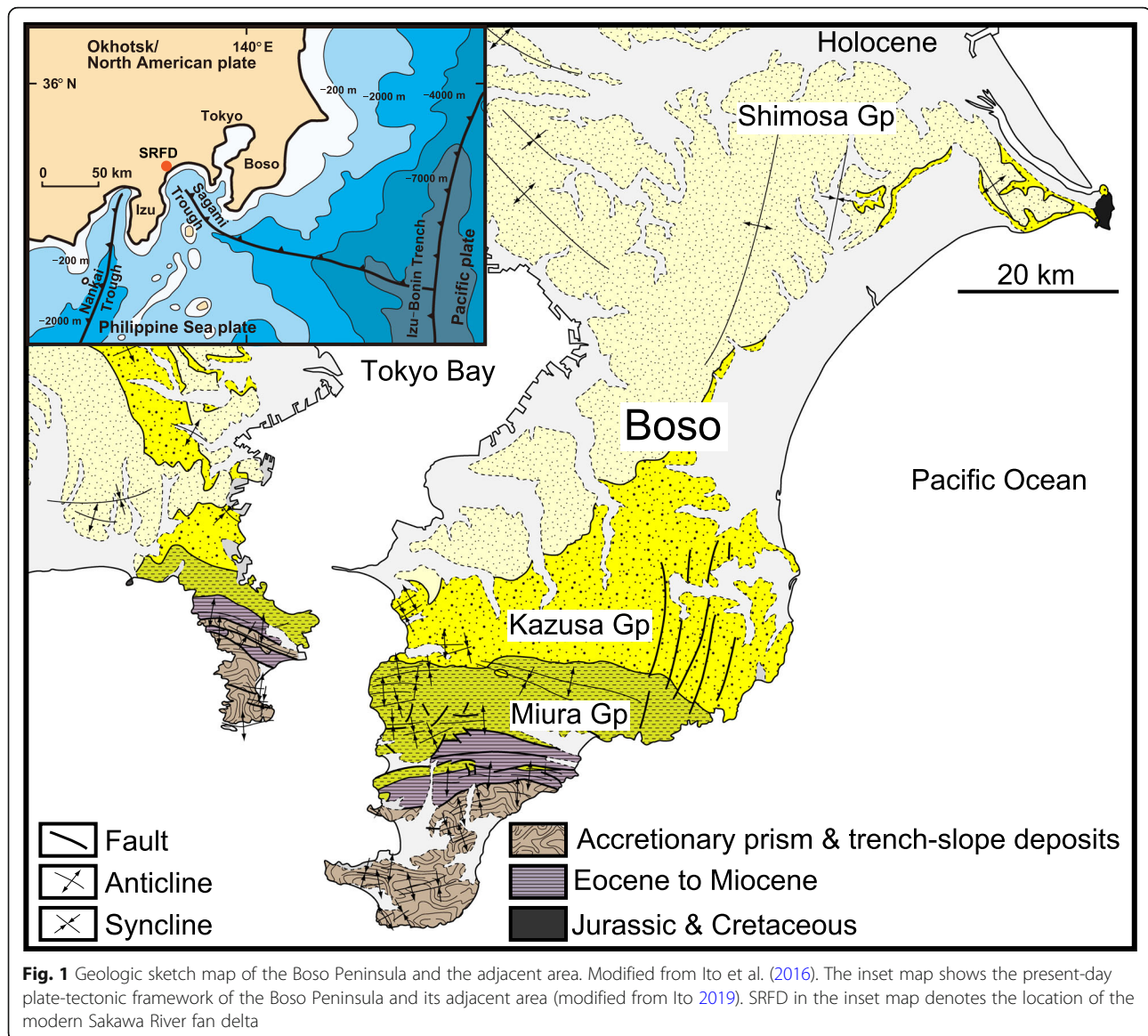Full list of author information is available at the end of the article

Introduction

Mapping of tephra key beds within heterogeneous siliciclastic successions can provide physically defined time lines for establishing detailed chronostratigraphic correlations of various types of lithofacies assemblages that document different depositional processes and environments. These physically defined chronostratigraphic markers enable identification of the synchronous or diachronous development of distinctive lithofacies assemblages, bounding surfaces, and depositional cycles in onshore outcrops (Ito 1995). In particular, the identification of local and regional synchroneity and diachroneity of stratigraphic cyclicities is crucial for elucidating spatial and temporal variations in the interaction between allogenic and autogenic controls (i.e., external and internal forces to the system, respectively, in the sense of Blum et al. 2018) on stratal formation within and between sedimentary basins. Tephra key beds are commonly intercalated in siliciclastic successions that are formed in active margin basins, such as forearc and backarc basins in the Japanese islands, and have been used for local and regional chronostratigraphic correlations and dating of both marine and nonmarine sedimentary successions (e.g., Machida and Arai 2011). These correlations and dating have enabled high-resolution analyses of the origins of stratigraphic cyclicities in terms of glacial and interglacial sea-level cycles, particularly during the Pliocene and Pleistocene (e.g., Ito and Katsura 1992; Sakai and Masuda 1996; Pickering et al. 1999).

A thick Pleistocene marine succession that is defined as the Kazusa Group (maximum thickness ~ 3000 m) is developed on the central part of the Boso Peninsula, central Japan (Figs. 1, 2, and S1). The group is characterized by high sedimentation rates (1.5 m/1000 year on average; Ito and Katsura 1992), and contains many tephra key beds, which have enabled high-resolution stratigraphic analyses of the group (e.g., Okada and Niitsuma 1989; Ito and Katsura 1992; Satoguchi 1995; Pickering et al. 1999; Tamura et al. 2019). Part of the muddy interval of this group in the Kokumoto Formation (the Chiba composite section) has been assigned as an international type section for the Lower–Middle Pleistocene Subseries boundary (the base of the Chibanian Stage (0.774 Ma: International Commission of Stratigraphy, 2020) (Kazaoka et al. 2015; Suganuma et al. 2018) (Figs. 2 and S1). The high-resolution stratigraphic framework for the Kazusa Group allows detailed analyses of the spatial and temporal variations in depositional systems in terms of relative sea-level changes, which are considered to have been controlled primarily by glacioeustasy (Ito and Katsura 1992). However, the relative timing of different types of depositional systems, which formed in between coastal, shallow-marine, and deep-water environments, has not yet been precisely analyzed in terms of the depositional processes and development of lithofacies architecture from coastal and shallow-marine to deep-water systems.

In particular, the muddy interval that contains the Chiba composite section is underlain and overlain by deep-water deposits, which are characterized by the development of thick- to very thick-bedded (cf., Campbell 1967) sandstones in the Kokumoto Formation. These sandstones are commonly ungraded or weakly graded in the uppermost part of the beds and/or convoluted, and can be classified as deep-water massive sandstones (DWMSs) (in the sense of Stow and Johansson 2000). DWMSs similar to those in the Kokumoto Formation are also developed in the upper Umegase and Chonan formations of the Kazusa Group. Although DWMSs are considered to be important reservoirs in many hydrocarbon systems worldwide (Stow and Mayall 2000), their origins and depositional processes still remain controversial (Stevenson and Peakall 2010). In addition, DWMSs, as well as other types of sandstone beds formed in deep-water environments, are generally interpreted to have been formed by sediment gravity flows (*sensu lato*), which are an important type of underwater flows and move huge amounts of sediments on Earth (Talling et al., 2013b). These flows are also interpreted to have been responsible for the fluctuations in the carbon budget and storage in the deep-water environments through time, and therefore have played an important role in modulating CO_2 levels in the atmosphere (Galy et al. 2007; Talling et al., 2013b; Hodgson et al. 2018). A better understanding of the origins of DWMSs in the Kazusa Group can constrain one type of variations in the possible processes and timing of active delivery of sands, which may also have been associated with the supply of organic carbon, into deep-water environments. Understanding of DWMSs is also crucial for establishing an accurate depositional framework for the development of the Chiba composite section that contains the Lower–Middle Pleistocene Subseries boundary (the base of the Chibanian Stage) in the group.

The major objective of the present study is to clarify the origins of thick- to very thick-bedded sandstones that can be identified as DWMSs in the Kazusa Group in relation to coeval coastal and shallow-marine deposits on the basis of the chronostratigraphic framework that is defined by the mapping of tephra key beds. In particular, one aim of the study is to clarify the relative timing of the active delivery of coarse-grained sediments beyond the shelf margin to develop DWMSs within the framework of the oxygen isotopic sea-level index.

Fig. 1 Geologic sketch map of the Boso Peninsula and the adjacent area. Modified from Ito et al. (2016). The inset map shows the present-day plate-tectonic framework of the Boso Peninsula and its adjacent area (modified from Ito 2019). SRFD in the inset map denotes the location of the modern Sakawa River fan delta
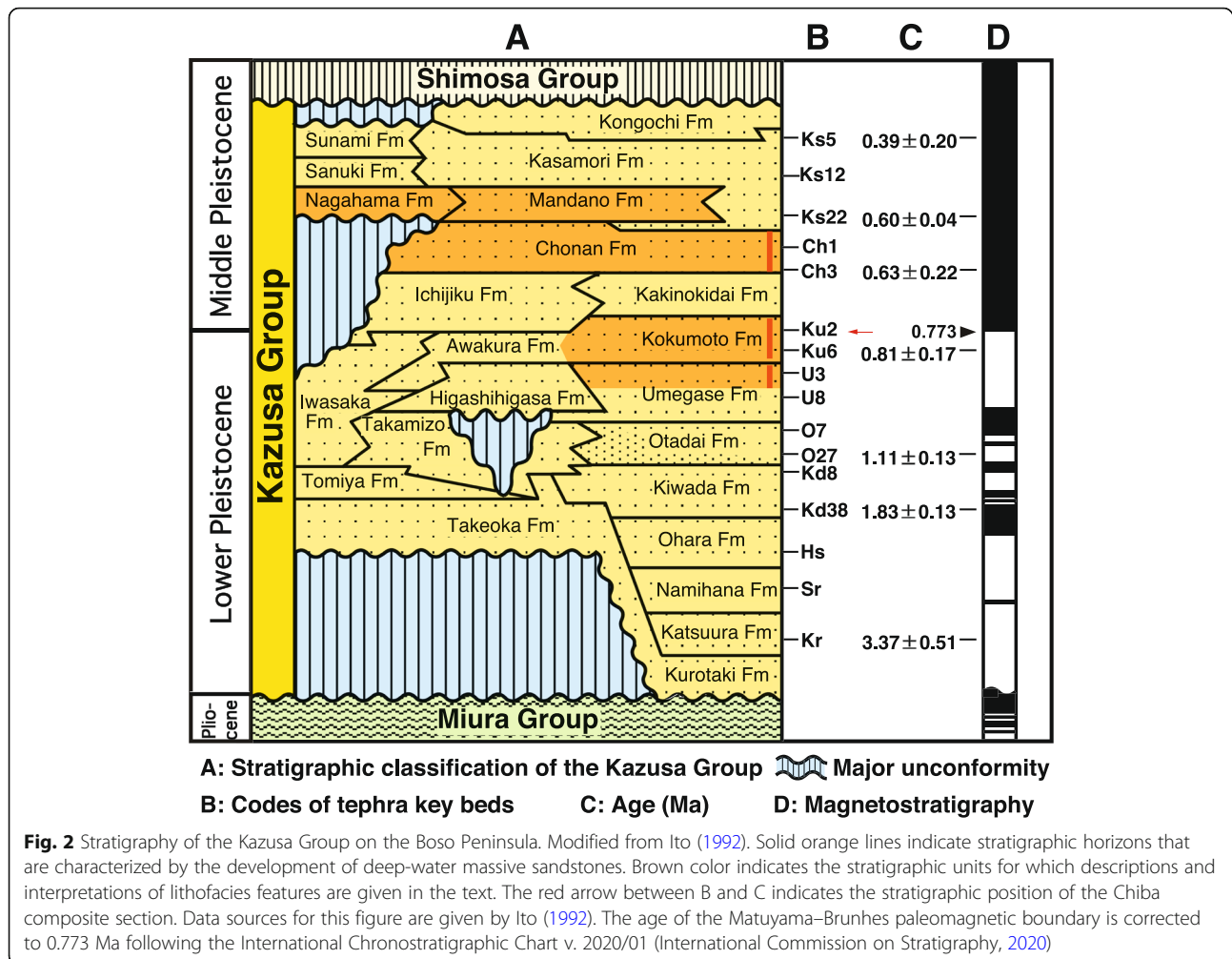
Geologic setting

The Kazusa Group is an infill of the Pleistocene Kazusa forearc basin. The basin is interpreted to have developed in response to the west-northwestward subduction of the Pacific plate beneath the Eurasia plate (later the Okhotsk/North American plate; Nakajima and Hasegawa 2010) along the Izu–Bonin trench, which was superimposed by the northwestward subduction of the Philippine Sea plate beneath the Eurasia plate along the Sagami trough between 2.4 and 0.45 Ma (Ito and Masuda 1988; Ito and Katsura 1992) (Fig. 1). The lower part of the group is characterized by deep-water basin plain, submarine-fan, and lower-slope deposits in the northeastern downslope area, and by upper-slope and outer-shelf deposits in the southwestern upslope area (Ito and Katsura 1992) (Fig. S1). In contrast, upper-slope

and outer-shelf deposits are widely developed in the upper part of the group, in association with minor inner-shelf and coastal deposits in the southwestern upslope area (Fig. S1). The lithofacies succession of the entire Kazusa Group has been classified into 17 high-frequency depositional sequences, which are considered to have been controlled primarily by glacioeustatic sea-level changes that were superimposed on the forearc tectonics, and which comprise transgressive and highstand sequence sets of a third-order composite sequence with a duration of about 1.95 Myr. (Ito and Katsura 1992).

DWMSs are developed in several stratigraphic horizons of the upper Umegase, Kokumoto, and Chonan formations of the Kazusa Group, in ascending order (Fig. 2). These DWMS-containing stratigraphic horizons are hereafter defined as packets: PU1 and PU2 in the upper

Fig. 2 Stratigraphy of the Kazusa Group on the Boso Peninsula. Modified from Ito (1992). Solid orange lines indicate stratigraphic horizons that are characterized by the development of deep-water massive sandstones. Brown color indicates the stratigraphic units for which descriptions and interpretations of lithofacies features are given in the text. The red arrow between B and C indicates the stratigraphic position of the Chiba composite section. Data sources for this figure are given by Ito (1992). The age of the Matuyama–Brunhes paleomagnetic boundary is corrected to 0.773 Ma following the International Chronostratigraphic Chart v. 2020/01 (International Commission on Stratigraphy, 2020)
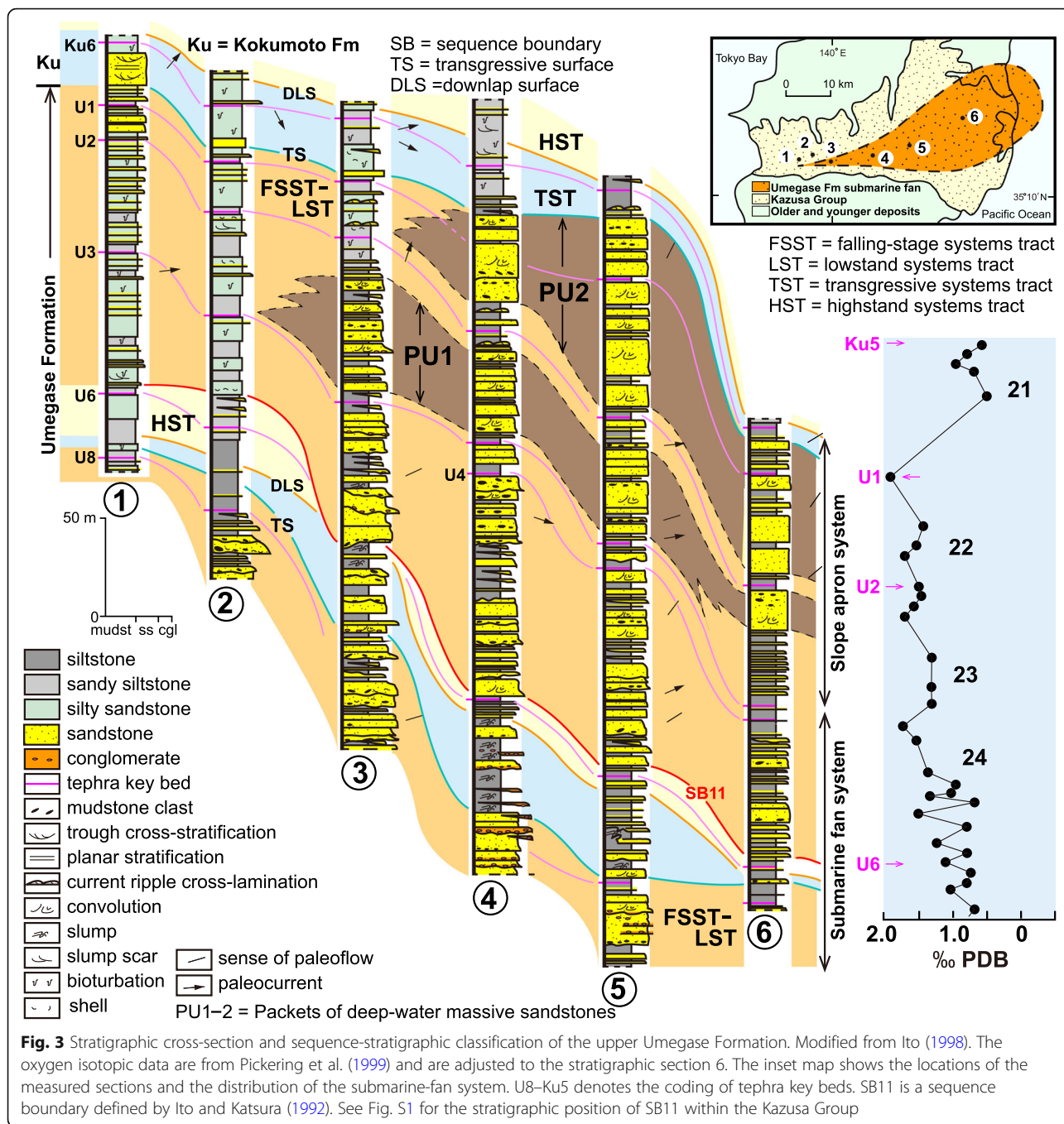
Umegase Formation; PK1 and PK2 in the Kokumoto Formation; and PC1–PC4 in the Chonan Formation (Figs. 3, 4, and 5a). In general, each packet is defined by abrupt replacement of muddy deposits with thick- to very thick-bedded sandstones at the base and also by an abrupt change from thick- to very thick-bedded sandstones to muddy deposits at the top, although some thick- to very thick-bedded sandstones show abrupt changes in thickness in the upslope and/or downslope directions (Figs. 3, 4, and 5a). Downslope correlation of the base and top of each packet is also supported by the correlation of some tephra key beds that are intercalated in muddy deposits between the packets. The first occurrence of PU1 in the upper Umegase Formation coincides with the abandonment of a submarine canyon–submarine fan system in the Kazusa Group, and occurred after the deposition of the U3 tephra key bed (Ito 1998; Ito and Saito 2006) (Fig. 3). The submarine canyon is interpreted to have been about 8 km long, up to 1 km wide, and more than 100 m deep (Ito and Saito 2006), and is considered to have acted as a conduit for northeastward-flowing

turbidity currents and other types of sediment gravity flows from which submarine-fan deposits (the Otadai and Umegase formations) with a maximum thickness of 1050 m formed between ca 1.2 and ca 0.8 Ma (Hirayama and Nakajima 1977) (Figs. 2 and S1).

Even after the abandonment of the submarine canyon in the Kazusa forearc basin, active shedding of coarse-grained sediments into the upper-slope or deeper environments eventually occurred, particularly during the falling and lowstand stages (Ito 1992, 1998). This sediment shedding might have also facilitated the development of the packets in the three formations.

Methods/experimental

We conducted detailed outcrop analyses of the upper Umegase, Kokumoto, and Chonan formations and of the coeval coastal and shallow-marine deposits of the Chonan Formation, such as the Mandano and Nagahama formations on the central part of the Boso Peninsula, Japan. In particular, we conducted detailed descriptions and interpretations of

Fig. 3 Stratigraphic cross-section and sequence-stratigraphic classification of the upper Umegase Formation. Modified from Ito (1998). The oxygen isotopic data are from Pickering et al. (1999) and are adjusted to the stratigraphic section 6. The inset map shows the locations of the measured sections and the distribution of the submarine-fan system. U8–Ku5 denotes the coding of tephra key beds. SB11 is a sequence boundary defined by Ito and Katsura (1992). See Fig. S1 for the stratigraphic position of SB11 within the Kazusa Group

the lithofacies features of each formation in outcrops to establish the depositional processes and depositional environments of each formation on the basis of the facies analysis methodology. Some sediment samples were also collected from the outcrops to analyze vertical changes in grain sizes within sandstone beds using a laser diffraction grain size analyzer (Malvern Mastersizer 3000) at Niigata University, Japan. In addition, we also conducted sequence-stratigraphic analyses of the formations along with the oxygen isotopic sea-level index of the formations to assess

spatial and temporal variations in the timing of active delivery of coarse-grained sediments beyond the shelf margin, which may have been responsible for the development of DWMSs.

Results

Relationships between the packets and coeval shallow-marine and coastal deposits

Because the stratigraphic units that contain the packets record an overall regression within the highstand
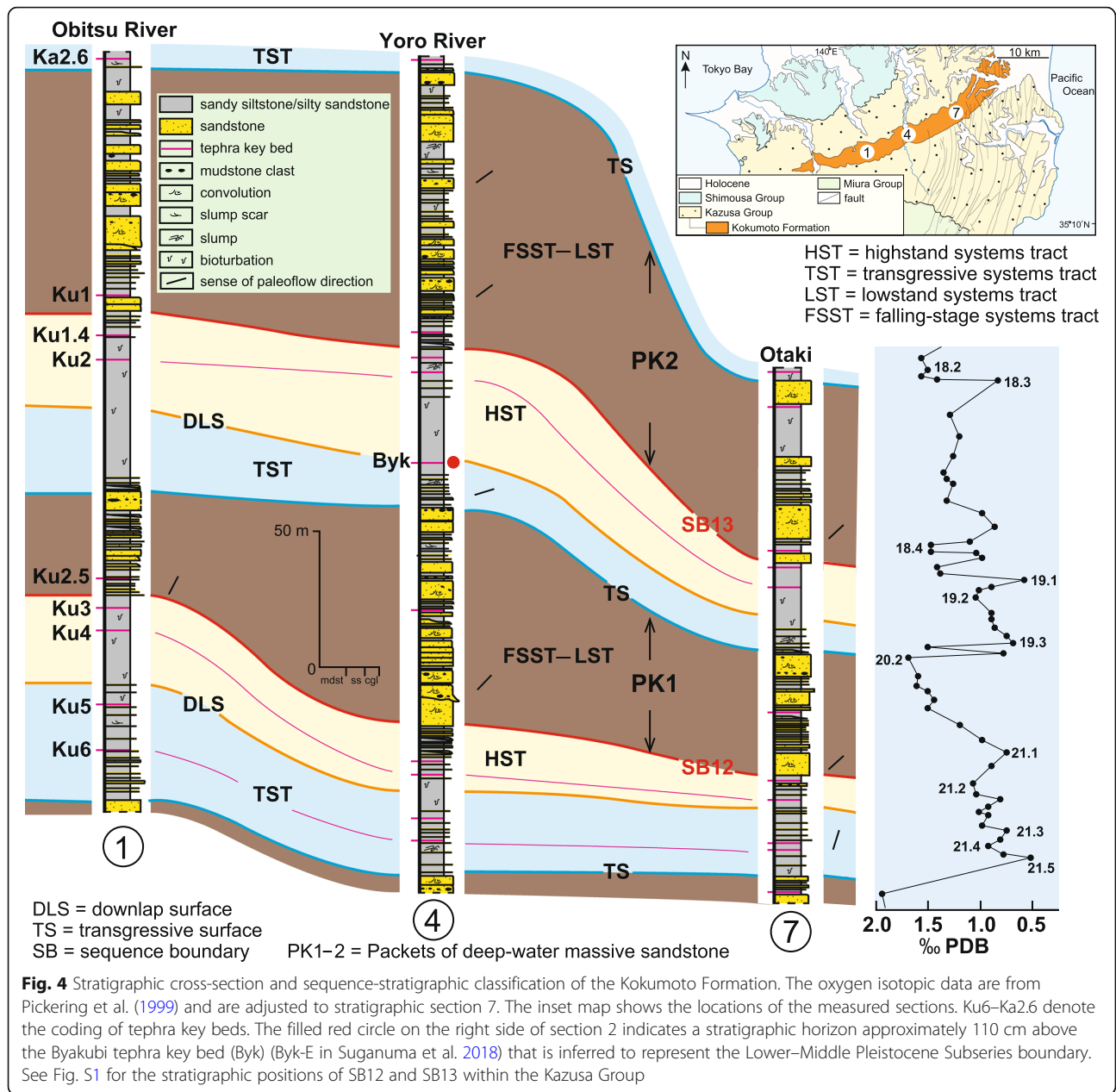
Fig. 4 Stratigraphic cross-section and sequence-stratigraphic classification of the Kokumoto Formation. The oxygen isotopic data are from Pickering et al. (1999) and are adjusted to stratigraphic section 7. The inset map shows the locations of the measured sections. Ku6–Ka2.6 denote the coding of tephra key beds. The filled red circle on the right side of section 2 indicates a stratigraphic horizon approximately 110 cm above the Byakubi tephra key bed (Byk) (Byk-E in Suganuma et al. 2018) that is inferred to represent the Lower–Middle Pleistocene Subseries boundary. See Fig. S1 for the stratigraphic positions of SB12 and SB13 within the Kazusa Group
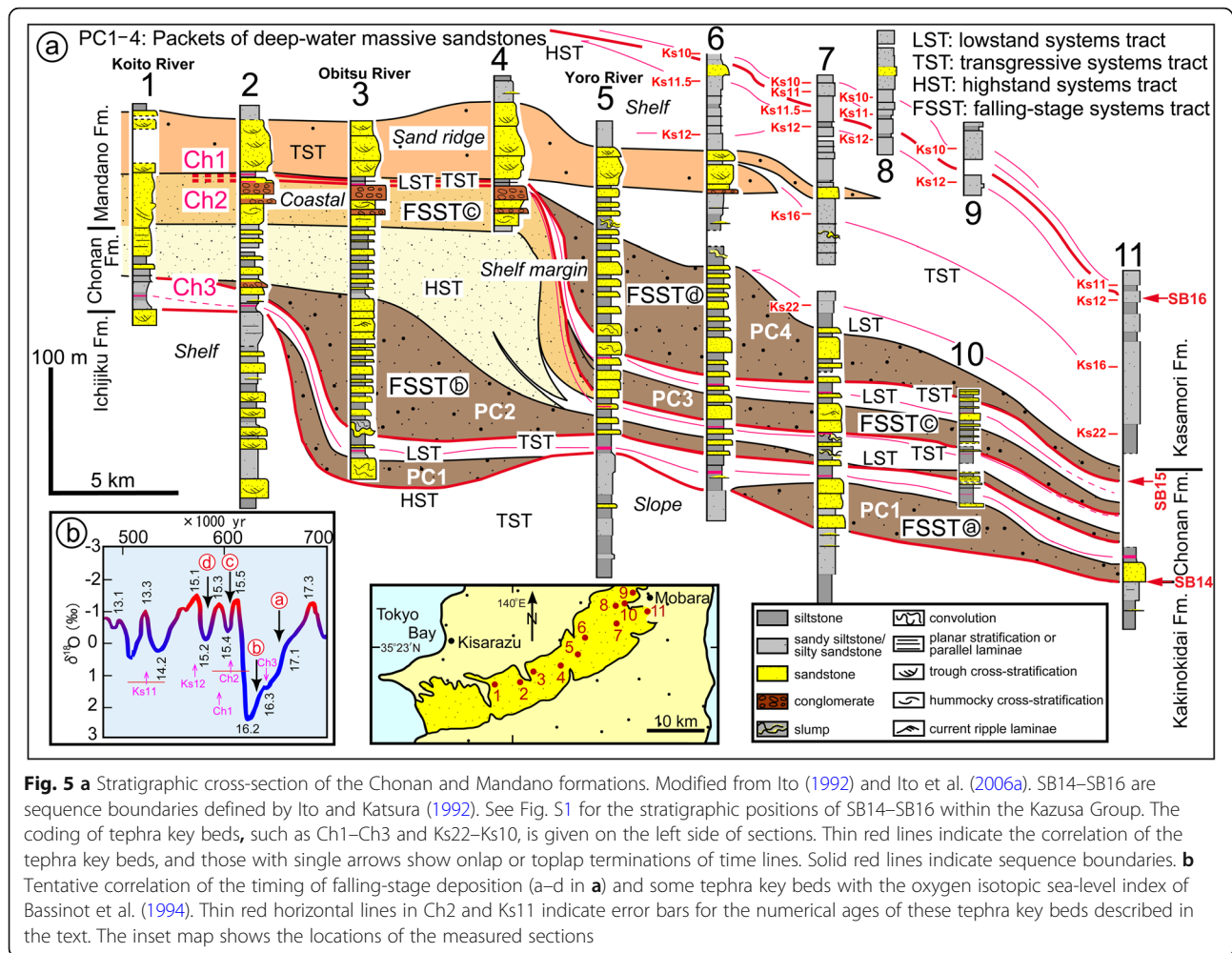
sequence set of the third-order composite sequence of the Kazusa Group (Ito and Katsura 1992), PC1–PC4 in the Chonan Formation have the highest potential for clarifying the sequence-stratigraphic relationships between the development of the packets (PC1–PC4) and that of coeval shallow-marine and coastal deposits. PU1–PU2 and PK1–PK2, for which coeval coastal deposits are not exposed in outcrop on the Boso Peninsula (Fig. S1), are not suitable for this purpose. Consequently, we first examine the relationship between PC1–PC4 and coeval shallow-marine and coastal deposits (the Mandano and Nagahama formations) in the southwestern upslope areas (Figs. 2 and 5a).

Lithofacies features of the Chonan, Mandano, and Nagahama formations

Descriptions and interpretations of the major lithofacies features of the Chonan, Mandano, and Nagahama formations have been given elsewhere (Ito 1992; Ito and Katsura, 1992; Ito et al. 2006a; Fuse et al. 2013). Here, we expand on previous studies and describe the distinctive lithofacies features of these formations to clarify the relationship between PC1–PC4 and their coeval coastal and shallow-marine deposits.

Chonan Formation

The Chonan Formation consists of interbedded very fine- to medium-grained sandstones, silty sandstones,

Fig. 5 a Stratigraphic cross-section of the Chonan and Mandano formations. Modified from Ito (1992) and Ito et al. (2006a). SB14–SB16 are sequence boundaries defined by Ito and Katsura (1992). See Fig. S1 for the stratigraphic positions of SB14–SB16 within the Kazusa Group. The coding of tephra key beds, such as Ch1–Ch3 and Ks22–Ks10, is given on the left side of sections. Thin red lines indicate the correlation of the tephra key beds, and those with single arrows show onlap or toplap terminations of time lines. Solid red lines indicate sequence boundaries. **b** Tentative correlation of the timing of falling-stage deposition (a–d in **a**) and some tephra key beds with the oxygen isotopic sea-level index of Bassinot et al. (1994). Thin red horizontal lines in Ch2 and Ks11 indicate error bars for the numerical ages of these tephra key beds described in the text. The inset map shows the locations of the measured sections
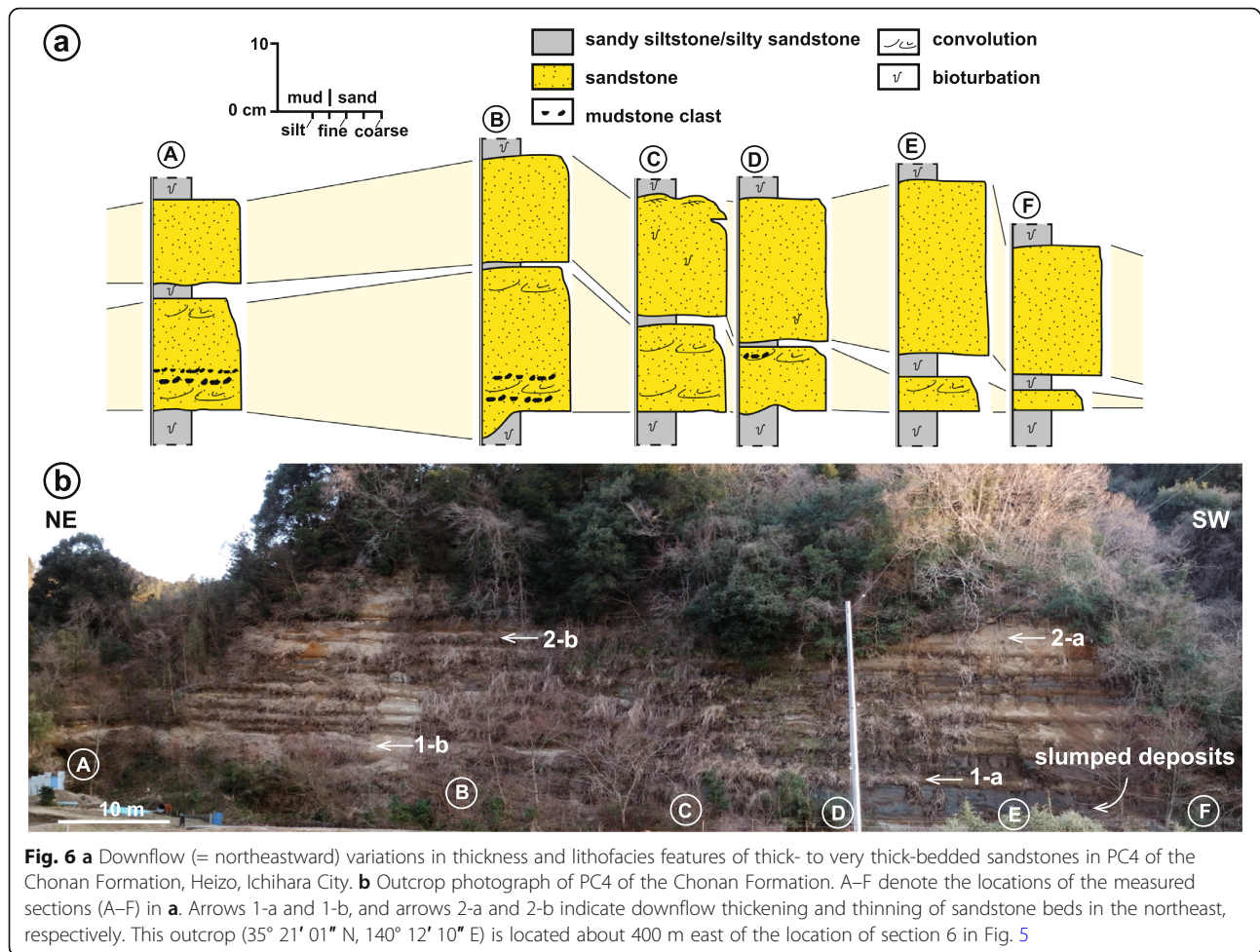
and sandy siltstones, and is up to 170 m thick (Figs. 5, 6, and S2a). The sandstone beds generally have a lenticular geometry and show compensation stacking (Fig. 6). Internally, these beds are either ungraded, ungraded with normal grading in the uppermost part, or entirely normally graded (Fig. S2b–c). In addition, inverse-to-normal grading, or alternation of inverse and normal grading is also observed in some sandstone beds (Fig. S2d–e). Parallel lamination and current-ripple cross-lamination are also developed in the sandstone beds, except in ungraded or some normally graded sandstones (Fig. S2e–f). Normally graded sandy siltstones with carbonaceous fragments commonly rest on the top of normally graded sandstones, particularly in the northeastern downslope area (Fig. S2c). Minor hummocky cross-stratification and dune structures are also observed in some sandstone beds, particularly those formed in the southwestern upslope area, where the formation unconformably overlies the Ichijiku Formation (Figs. 2 and S2g–h). Ungraded or ungraded and normally graded (in the uppermost part) sandstones are commonly one or more meters thick and

contain convolute bedding and mudstone clasts. Locally, the interbeds also exhibit slump structures (Fig. 6b). In addition, the Chonan Formation is characterized by the occurrence of cold-water molluscan shell and benthic foraminifer assemblages that indicate outer-shelf to upper-slope environments (ca. 50–300 m paleowater depth; Baba 1990; Kitazato 1997). The formation is moderately to intensely bioturbated with *Rosselia-*, *Thalasinoides-*, and *Teichichnus*-type burrows. Three tephra key beds (Ch1, Ch2, and Ch3, in descending order) are intercalated in sandy siltstones or silty sandstones (Figs. 5a and S2a–b). Four packets (PC1–PC4) with thick- to very thick-bedded sandstones are developed below and above the muddy deposits that contain the three tephra key beds (Fig. 5a).

Mandano Formation

The Ch1 and Ch2 tephra key beds are also intercalated in the Mandano Formation, the outcrops of which are developed in the farther southwestern upslope area from the outcrops of the Chonan

Fig. 6 a Downflow (= northeastward) variations in thickness and lithofacies features of thick- to very thick-bedded sandstones in PC4 of the Chonan Formation, Heizo, Ichihara City. **b** Outcrop photograph of PC4 of the Chonan Formation. A–F denote the locations of the measured sections (A–F) in **a**. Arrows 1-a and 1-b, and arrows 2-a and 2-b indicate downflow thickening and thinning of sandstone beds in the northeast, respectively. This outcrop (35° 21′ 01″ N, 140° 12′ 10″ E) is located about 400 m east of the location of section 6 in Fig. 5

Formation (Machida et al. 1980), where the formation is also underlain by the lower part of the Chonan Formation, which contains the Ch3 tephra key bed (Figs. 5a, 7, and S3a). The Mandano Formation is characterized by medium- to very coarse-grained sandstones and pebbly sandstones, and pebble-sized conglomerates (Figs. 5a, 7, and S3b–d). The formation is informally subdivided into lower, middle, and upper parts, with the middle part being characterized by muddy deposits (0–17 m thick) (Figs. 7 and S4a).

The lower Mandano Formation, which has a maximum thickness of 50 m, shows an overall coarsening-upward succession. The lower section contains very fine- to medium-grained sandstones that show planar stratification and trough cross-stratification, and minor hummocky cross-stratification, and local intercalation with silty sandstones. The middle section comprises fine- to very coarse-grained sandstones that show planar stratification and trough cross- and hummocky cross-stratification, in association with wave-ripple lamination, and intercalation with pebble- to granule-sized conglomerates that also display planar stratification and trough cross- and wave-ripple cross-stratification. Finally, the upper section contains pebble- to granule-sized conglomerates (Figs. 7, S3d, and S4a). The basal contact with the underlying Chonan Formation is sharp but locally erosional (Figs. 7 and S3a). In addition, the lower section locally shows inclined bedding exhibiting a downlap termination to the upper Chonan Formation (i.e., clinoform), discordance of bedding, and some scours up to 5 m deep (Figs. 7 and S3b–c). The lower part of the conglomerates in the upper section is characterized by trough cross-stratification and local intercalations of planar stratified and trough cross-stratified, medium- to very coarse-grained sandstones (Figs. 7 and S4a). The basal contact of the lower part of the conglomerates with the underlying sandy deposits of the middle section is generally sharp or slightly erosional and is marked by a distinct grain size break (Fig. S3d). The upper part of the conglomerates in the upper section is characterized by planar stratification, which originally gently inclined in the northeastern offshore direction, and by preferred clast imbrication inclined in the northeastern offshore direction.
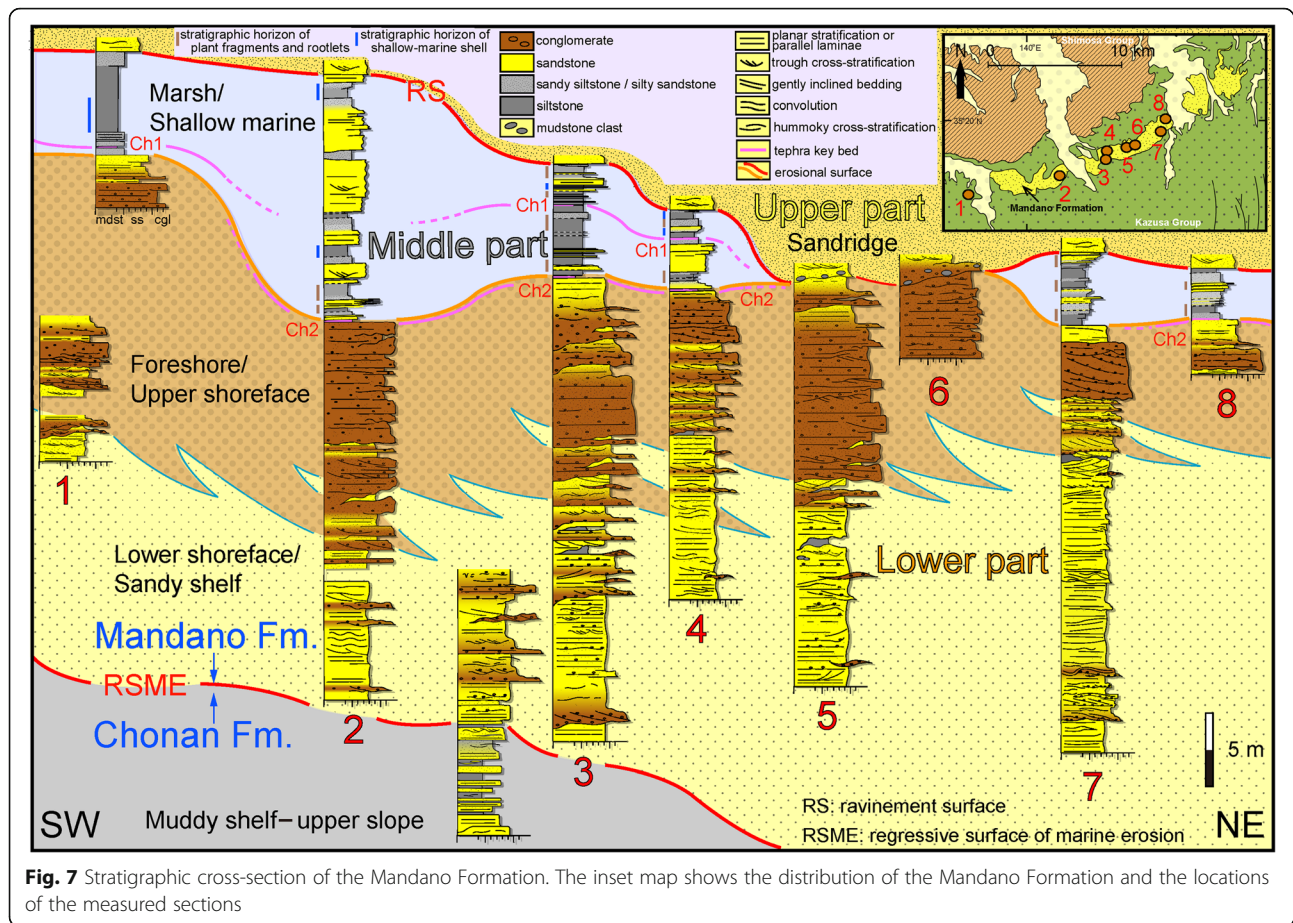
Fig. 7 Stratigraphic cross-section of the Mandano Formation. The inset map shows the distribution of the Mandano Formation and the locations of the measured sections

The conglomerates are locally overlain by fine- to medium-grained sandstones with wavy stratification, rootlets, and burrows. The Ch2 tephra key bed is intercalated in the uppermost part of the upper section of the lower Mandano Formation (Figs. 7 and S4a).

The middle Mandano Formation is represented by muddy deposits that lie on an erosional basal surface incised into the lower Mandano Formation (locally up to 1 m deep) (Figs. 7 and S4a). The muddy deposits are sandy siltstones and silty sandstones and commonly contain leaf and wood fragments, with locally developed rootlets (Fig. 7). In addition, very fine- to medium-grained sandstones with planar stratification and trough cross-stratification, and heterolithic bedding, which locally exhibit parallel lamination and current-ripple cross-lamination, also occur within the muddy deposits (Fig. 7). Overall, both the muddy deposits and the intercalated sandy deposits are moderately to intensely bioturbated. The Ch1 tephra key bed is intercalated in the middle part of the muddy deposits (Machida et al. 1980), where finer-grained muddy deposits are dominant and shallow-marine and embayment molluscan shells, such as *Raetellops pulchellus* and *Macoma incongrua*, are found, particularly in a horizon lying mainly above the Ch1 tephra

key beds (Figs. 7 and S4a–b). Locally, intercalations of carbonaceous fragments increase in abundance again upsection in the muddy deposits. The thickness of the middle Mandano Formation varies from 0 to 17 m, consistent with the amount of erosion at the base of the upper Mandano Formation (Fig. 7).

The upper Mandano Formation shows an overall convex-up, lenticular geometry, is up to 70 m thick (Fig. 5a), and consists of medium- to very coarse-grained sandstones and pebbly sandstones that are characterized by trough cross-stratification (height up to 4 m) and minor planar stratification (Fig. S4c). These deposits commonly have bioturbation structures with *Ophiomorpha-*, *Thalassinoides-*, and *Skolithos*-type burrows, and contain shallow-marine molluscan shells (Fig. S4d) that are interpreted to indicate a paleowater depth of 30–250 m (Baba 1990), as well as bone fragments of marine mammals. The upper Mandano Formation fines upward to muddy deposits of the Kasamori Formation, which contains the Ks12 tephra key bed in a horizon just above the top of the upper Mandano Formation (Tokuhashi and Endo 1984) (Fig. 5a), and includes very fine- to medium-grained sandstones that lack any wave-built sedimentary structures. The trough cross-stratification

of the upper Mandano Formation generally indicates eastward–northeastward-directed paleocurrents, and the upper Mandano Formation pinches out into the middle part of the Kasamori Formation in the northeastern downslope area (Fig. 5a), where sandy siltstones and silty sandstones are dominant and are intercalated with very fine- to coarse-grained sandstone beds and contain molluscan shells that indicate a paleowater depth of 50–300 m (Baba 1990).

Nagahama Formation

The upper Mandano Formation has been correlated with the Nagahama Formation (Machida et al. 1980; Mitsunashi 1990; Ito 1992; Nakajima and Watanabe 2005). The Nagahama Formation is developed mainly in the southwestern upslope area of the upper Mandano Formation (Fig. 2). The outcrops of the Nagahama Formation are about 1.8 km wide and about 6 km long in the northeastern downslope direction, and the formation has a distinct erosional basal surface that incises into the underlying Chonan and Ichijiku formations and also some older muddy deposits that are equivalent to the Kokumoto and Umegase formations (Nakajima and Watanabe 2005) (Fig. S5a–b). The Nagahama Formation contains a basal pebble-sized conglomerate that locally contains mudstone rip-up clasts up to 2 m long. The conglomerates fine upward to fine- to medium-grained, medium- to very thick-bedded, amalgamated sandstones and pebbly sandstones that commonly have convolute bedding, and finally to interbedded very fine- to very coarse-grained sandstones and sandy siltstones that are locally associated with slumped deposits, yielding a total thickness of up to 30 m (Fig. S5a–b). The conglomerates in the basal part of the formation show gently undulating waveforms in outcrops oriented nearly parallel to the northeastward-directed downslope direction, and also locally have gently inclined bedding in the northeast (Fig. S5a). In contrast, the conglomerates in outcrops oriented obliquely or orthogonally to the downslope direction show trough cross-stratification (Fig. S5b). Medium- to very coarse-grained sandstones and pebbly sandstones locally rest on the waveforms and internally contain gently undulating spaced stratification and/or ungraded or normally graded bedding (Fig. S5a). The formation fines upward to sandy siltstones of the Sanuki Formation, which are intercalated with the Sn15 tephra key bed that is equivalent to the Ks11.5 tephra key bed in the Kasamori Formation (Machida et al. 1980) (Figs. 5a and S1). The Nagahama Formation is overlain by the southwestern extension of the upper Mandano Formation; the contact between the two formations is a slight erosional surface (Fig. S5c).

Lithofacies organization of the packets

To clarify the origins of the packets in the upper Umegase, Kokumoto, and Chonan formations that contain thick- to very thick-bedded DWMSs, we investigated the common lithofacies features of the sandstone beds in the packets, incorporating the descriptions of lithofacies features of the Chonan Formation provided above, and their inferred formation processes. The lithofacies assemblages of the sandstone beds that constitute the packets contain six common lithofacies types (types 1–6), as summarized in Table 1. Types 1 and 2 characterize the packets and can be identified as DWMSs, in association with types 3–6. Types 3–6 are also found in muddy intervals; these intervals are characterized by bioturbated sandy siltstones and/or silty sandstones intercalated with very thin- to medium-bedded types 3–6 sandstone beds in the three formations.

Types 1 and 2 sandstone beds commonly show abrupt thinning into the other types in both depositional dip and strike directions (Figs. 8, 9, and 10). Some types 1 and 2 sandstone beds also locally contain several flow units that are separated by muddy deposits (Ito et al. 2006b) (Fig. 9). In a section oriented oblique to their paleocurrent directions in the northeast, some thinned sandstone beds can be farther correlated with thicker and coarser sandstone beds that formed in a more northeastern downslope area (Fig. 10). Types 3 and 4 sandstone beds show vertical changes in grain sizes and sedimentary structures that differ from those in sandstone beds, which have been interpreted as deposits from waning turbidity currents (i.e., the Bouma model: Bouma 1962; the Lowe model: Lowe 1982; Talling et al. 2012). Locally, type 4 sandstone beds contain internal erosional surfaces and siltstone streaks. Types 5 and 6 sandstone beds are mainly medium- to very thin-bedded (in the sense of Campbell 1967) (Table 1), and are also common in muddy deposits below and above the packets. Overall, the assemblages of the six types of sandstone beds in each packet do not show any distinct thinning- and fining-upward or thickening- and coarsening-upward patterns.

Discussion

Depositional environments of the Chonan, Mandano, and Nagahama formations

Chonan Formation

The Chonan Formation is interpreted to have formed in outer-shelf to upper-slope environments, which intermittently received an active supply of sandy sediment from the southwestern hinterlands via sediment gravity flows (Ito 1992; Ito and Katsura 1992; Fuse et al. 2013) (Fig. 11). Some sandstone beds show vertical changes in grain sizes and sedimentary structures that differ from those of the Bouma and Lowe models (Bouma 1962;

Table 1 Lithofacies types and their inferred depositional processes. The outcrop features of each lithofacies type are shown in Fig. S6.

Type 1 Ungraded sandstones with convolution
Thickness: 50 cm–up to more than 250 cm
Description: Medium- to coarse-grained sandstones with sharp and flat or locally distinct erosional bases. No distinct sedimentary structures are developed and convolute structures are common. Locally, internal erosion surfaces in association with mudstone clasts are developed, and scattered coarse- to very coarse-grained sands and granules are also locally observed.
Interpretation: Rapid fall out of suspended particles from locally erosional high-density turbulent flows, and/or recurrent fall out of suspended particles from sustained high-density gravity flows (Lowe 1982; Kneller and Branney 1995; Talling et al. 2012), in association with bypassing of sedimentation from wakes. Locally developed internal erosion surfaces and mudstone clasts suggest amalgamation of thinner component sandstone beds.

Type 2 Ungraded sandstones with normal grading in the uppermost part
Thickness: 50 cm–up to more than 250 cm
Description: Major lithofacies features are very similar to those of type 1 except for the development of normally graded sandstones up to 10 cm in the uppermost part. Graded sandstones are medium- to very fine-grained and locally contain parallel- and/or current ripple-laminations and convolute laminations.
Interpretation: Rapid fall out of suspended particles from locally erosional high-density turbulent flows, and/or recurrent fall out of suspended particles from sustained high-density gravity flows (Lowe 1982; Kneller and Branney 1995; Talling et al. 2012), in association with fall out of finer grained particles from wakes.

Type 3 Inverse-to-normally graded sandstones with current ripple- and parallel-laminations
Thickness: 20–40 cm
Description: Inverse-to-normally graded, medium- to very fine-grained sandstones, in association with current ripple- and/or parallel-laminations. The basal and upper surfaces of sandstone beds are sharp and flat, and locally upper contacts are gradational to interbedded sandy siltstones.
Interpretation: Invers-to-normal grading indicates waxing and waning of lower density gravity flows, possibly ignited by hyperpycnal flows (Mulder et al. 2003).

Type 4 Alternation of current ripple- and parallel-laminated sandstones
Thickness: 20–150 cm
Description: Multiple repetition of inverse-to-normally graded, medium- to very fine-grained sandstones in association with current ripple- and parallel-laminations. Structureless and/or normally graded, medium- to very fine-grained sandstones are also locally intercalated. Internal erosion surfaces and/or muddy streaks are also locally intercalated.
Interpretation: Alternation of current ripple- and parallel-laminations, in association with internal erosion surfaces and muddy streaks indicate multicycles of waxing and waning gravity flows, possibly induced by hyperpycnal flows and/or breaching of sandy substrates (Mastbergen and Van den Bergen 2003; Mulder et al. 2003)

Type 5 Structureless sandstones
Thickness: 3–30 cm
Description: Medium- to fine-grained sandstones without any distinct normal and/or inverse grading, and sedimentary structures, except for locally developed convolute laminations. Sharp and flat basal and upper surfaces are common, and some beds have distinct erosional bases and contain mudstone clasts in the basal parts.
Interpretation: Rapid sediment fall out of turbulent suspension in locally erosional gravity flows (Talling et al. 2012).

Type 6 Normally graded or parallel- and/or current ripple-laminated sandstones
Thickness: 3–50 cm
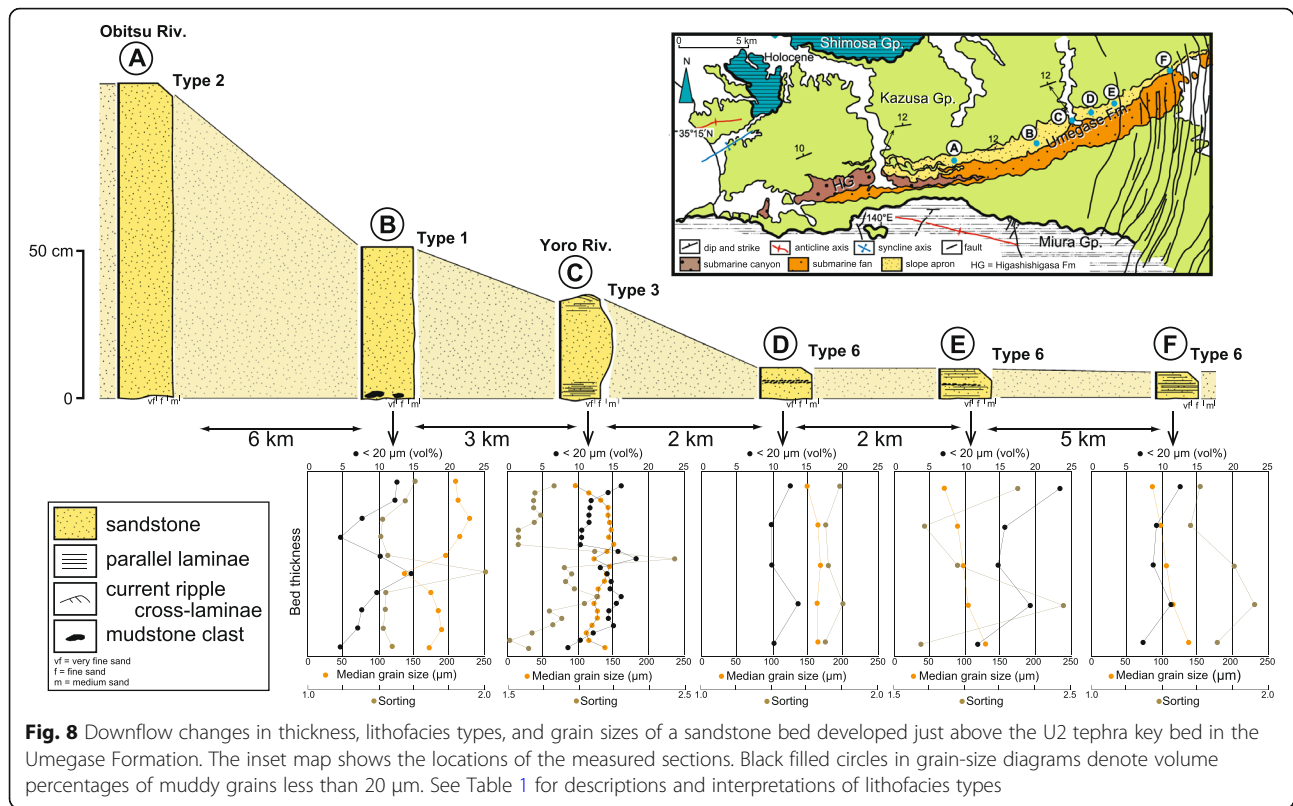Description: Medium- to very fine-grained sandstones with normal

Table 1 Lithofacies types and their inferred depositional processes. The outcrop features of each lithofacies type are shown in Fig. S6. *(Continued)*

grading in local association with parallel- and/or current ripple-laminations. Locally, this type sandstones fine upward to sandy siltstones that commonly contain carbonaceous fragments. Sharp and flat basal surfaces are common with locally developed distinct erosional basal surfaces. Mudstone clasts are included in the middle and upper parts of a single bed.
Interpretation: Locally erosive, waning, lower density turbidity currents (Talling et al. 2012). Carbonaceous fragments suggest an influence of hyperpycnal flows (Mulder et al. 2003; Zavala et al. 2006).

Lowe 1982), and are interpreted to have formed from unsteady turbidity currents, which exhibit temporal fluctuations in terms of waxing and waning of flow speeds (Kneller 1995). Hyperpycnal flows (in the sense of Mulder et al. 2003; Zavala et al. 2006) (Fuse et al. 2013) and/or breaching-induced turbidity currents (Mastbergen and Van Den Berg 2003) are considered to have been responsible for the development of unsteady turbidity currents. Thick- to very thick-bedded sandstones, which are ungraded or ungraded with normal grading in the uppermost part, are interpreted to have formed from rapid suspension fall out of sand particles from high-density sediment gravity flows (e.g., Lowe 1982; Talling et al. 2012) and/or continued suspension fall out of sand particles from quasi-steady and depletive turbidity currents (Kneller 1995). Normally graded sandy siltstones, which gradationally overlie graded sandstone beds, are interpreted to represent turbiditic muddy deposits (Talling et al. 2012), although laminated and ungraded muddy deposits, which also characterize muddy turbidites (Stow and Shanmugam 1980; Talling et al. 2012), are uncommon in the present examples. Locally observed hummocky cross-stratification in sandstone interbeds in the southwestern upslope area indicates the episodic influences of oscillatory current-dominated combined flows in an outer-shelf environment (e.g., Dumas et al. 2005), although the origin of hummocky cross-stratification remains disputed (Quin 2011; Morsilli et al. 2012).

Mandano Formation
The lower section of the lower Mandano Formation locally contains storm-wave-built sedimentary structures and is interpreted to have formed in a sandy inner-shelf environment, which is equivalent to, for example, the modern shelves around California and the Boso Peninsula (Clifton 2006; Nishida et al. 2019). The basal surface of the lower Mandano Formation is considered to have formed as a storm-wave-induced erosional surface in response to progradation of a sandy shelf system in association with offshore-directed migration of the storm wave base (Peters and Loss 2012) (Fig. 11a). Sandstones intercalated

Fig. 8 Downflow changes in thickness, lithofacies types, and grain sizes of a sandstone bed developed just above the U2 tephra key bed in the Umegase Formation. The inset map shows the locations of the measured sections. Black filled circles in grain-size diagrams denote volume percentages of muddy grains less than 20 μm. See Table 1 for descriptions and interpretations of lithofacies types

with conglomerates in the middle section of the lower Mandano Formation also contain distinctive storm-wave-built sedimentary structures and are interpreted to be lower shoreface deposits (Massari and Parea 1988; Hart and Plint 1989; Ito 1992; Ito et al. 2006b). The lower part of the conglomerates in the upper section of the lower Mandano Formation is considered to record the migration and aggradation of gravelly bars in an upper shoreface environment, whereas the upper part of the conglomerates may have formed in response to swash and backwash processes in a gravelly foreshore environment (Hart and Plint 1989; Clifton 2006; Bluck 2011). Locally observed fine- to medium-grained sandstones with wavy stratification, rootlets, and burrows in the uppermost part of the upper section are interpreted to have formed as eolian dune deposits in a backshore environment (Clifton 2006). The sharp and locally erosional basal contact of the upper shoreface deposits is considered to have formed by the migration of a gravel bar and trough system in an upper shoreface environment and is equivalent to a surf diastem (in the sense of Swift et al. 2003).

The distinct erosional basal surface of the middle Mandano Formation suggests an unconformity that was developed in response to a fall in relative sea level. This relative sea-level fall may have induced

preceding forced regression to form the lower Mandano Formation before the development of the basal unconformity of the middle Mandano Formation. The muddy deposits with carbonaceous fragments and rootlets overlying the erosional surface are considered to have formed in response to the reduction in coarse-grained sediment supply during the ensuing transgression. The muddy deposits in the middle Mandano Formation are interpreted to have formed initially in an estuary associated with mudflats and salt-marsh environments, which might have been affected by subsequent inundation of seawater to develop a shallow-marine muddy embayment (e.g., Allen 1997; Davidson-Arnott 2010) (Fig. 11c). The development of heterolithic bedding in the muddy deposits suggests reduced wave processes or the influence of tidal processes in the estuary (e.g., Boyd et al. 2006; Ahokas et al. 2014). Because the coastal gravelly deposits are considered to have been formed by active wave processes, longshore currents may have played an important role in alongshore transportation of coarse sediments to form spits at a river mouth (Burningham 2015) (Fig. 11c). The shallow-marine muddy embayment that was documented in the middle Mandano Formation appears to have formed in response to the development of gravelly spits (see Hiroki and Masuda 2000; Nielsen and Johannessen 2008;
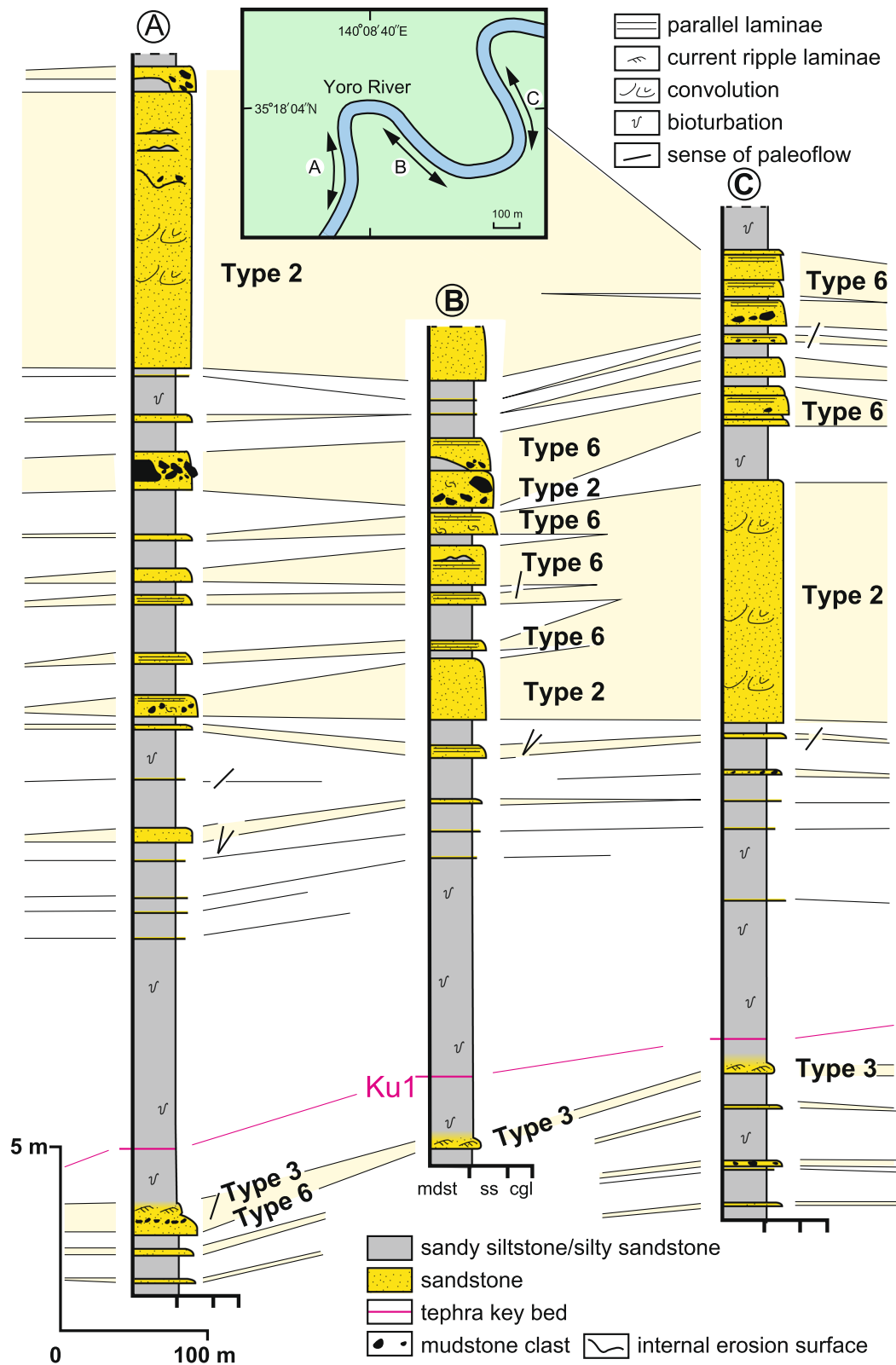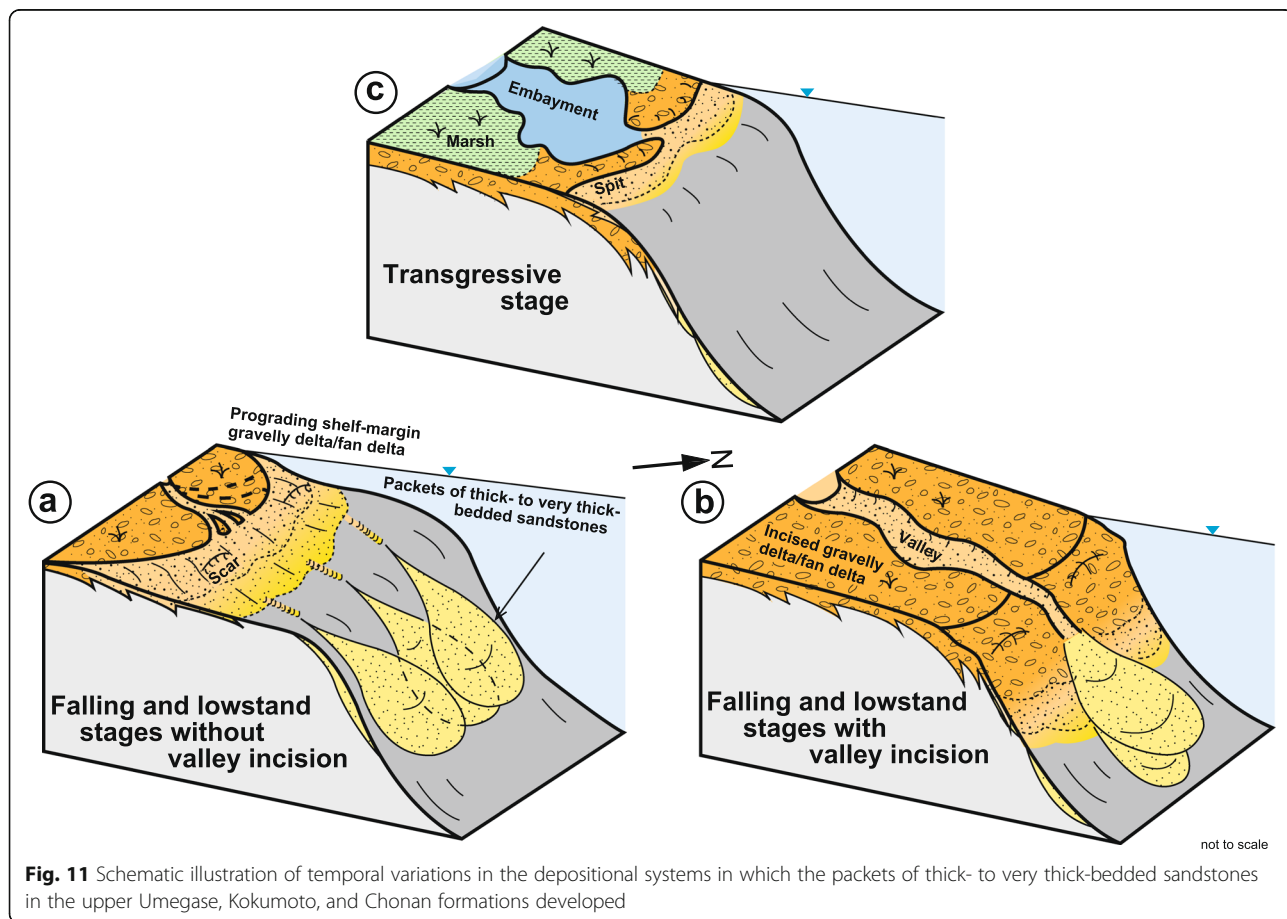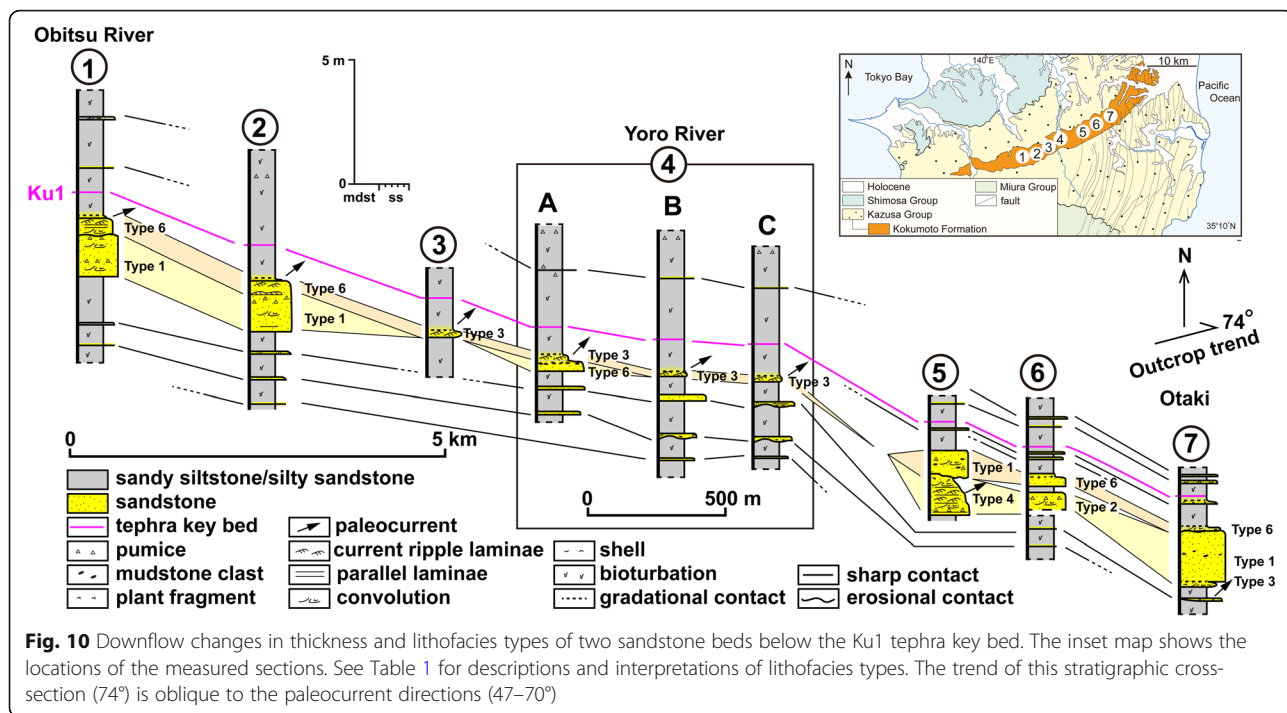
Fig. 9 Downflow changes in lithofacies types of sandstone beds above the Ku1 tephra key bed in PK2 of the Kokumoto Formation along the Yoro River (Location 4 in Fig. 4). The inset map shows the locations of the measured sections. See Table 1 for descriptions and interpretations of lithofacies types

Fig. 10 Downflow changes in thickness and lithofacies types of two sandstone beds below the Ku1 tephra key bed. The inset map shows the locations of the measured sections. See Table 1 for descriptions and interpretations of lithofacies types. The trend of this stratigraphic cross-section (74°) is oblique to the paleocurrent directions (47–70°)

Fig. 11 Schematic illustration of temporal variations in the depositional systems in which the packets of thick- to very thick-bedded sandstones in the upper Umegase, Kokumoto, and Chonan formations developed

Takao *et al. Progress in Earth and Planetary Science* (2020) 7:37

Page 15 of 21

Bartholdy et al. 2017), although distinct platform foresets that indicate the migration of gravelly spits are not observed in the present outcrop belt.

An overall convex-up lenticular geometry, unidirectional paleocurrents, and downslope termination into the Kasamori Formation, which is considered to have formed in an outer-shelf environment, indicate that the upper Mandano Formation represents shelf sand-ridge deposits formed by an overall transgression (Ito 1992). The basal erosional surface of the upper Mandano Formation represents a ravinement surface, and the development of the sand-ridge deposits is interpreted to have been influenced by the northeastward-directed intrusion of the paleo-Kuroshio Current into the Kazusa forearc basin in response to glacioeustatic sea-level rise (Ito 1992).

Nagahama Formation

The basal erosional surface of the Nagahama Formation and the overlying conglomerates indicate that the deposition of this formation was influenced by preceding erosion by sediment gravity flows in shelf and shelf-margin environments and the subsequent deposition in response to downslope migration and aggradation of gravelly bedforms from high-density gravity flows (cf., Ito 2019). The shallow incision of its base and its thin stratigraphic thickness may indicate that the Nagahama Formation was formed as an infill of a shallow valley on an outer-shelf and/or shelf margin (Ito 1992; Ito et al. 2006a) (Fig. 11b). An overall fining-upward pattern in the entire Nagahama Formation is considered to have been formed by backfilling of the valley in response to an overall rise in relative sea level.

Sequence stratigraphy of the Chonan, Mandano, and Nagahama formations

The Chonan Formation is interpreted to have formed mainly during the marine isotopic stage (MIS) 16 (Okada and Niitsuma 1989; Pickering et al. 1999), and the Ch2 tephra key bed has yielded a zircon U–Pb age of 0.61 ± 0.02 Ma (Ito et al. 2017). In addition, the Ks11 tephra key bed in the Kasamori Formation is interpreted to have formed during MIS 13.3 (in the sense of Bassinot et al. 1994) (0.52 ± 0.02 Ma) (Shirai 2001). A stratigraphic horizon between the Ks11 and Ks 12 tephra key beds, which are intercalated in muddy deposits that developed over the sand-ridge deposits of the upper Mandano Formation, was assigned as a sequence boundary (SB16 in Ito and Katsura 1992). The present interpretation of lithofacies architecture and bounding surface features (such as the sharp base of the lower Mandano Formation, the erosional bases of both the middle and upper Mandano Formation, and the reinterpretation of the stratigraphic relationship between the Nagahama

and upper Mandano formations), together with the revised age framework of the Chonan, Mandano, and Nagahama formations, enable the three formations to be subdivided into four distinctive depositional stages in terms of higher-frequency sequence stratigraphy compared to the previous interpretation of Ito and Katsura (1992) (Figs. 5b and S1).

The development of four packets (PC1–PC4) is considered to have been induced by active shedding of coarse-grained clastic particles by both low-density and high-density sediment gravity flows into shelf-margin to upper-slope environments during the falling and lowstand stages of relative sea-level changes (Ito 1992, 1995; Ito and Katsura 1992) (Fig. 11a). Sandstone beds coarser than medium grain size, such as the types 1 and 2 beds, are considered to have formed from high-density gravity currents (Mulder and Alexander 2001; Talling et al. 2012).

The muddy horizon that is intercalated with the Ch3 tephra key bed is interpreted to have formed during MIS 16 (Nanayama et al. 2016). This muddy horizon is encased between PC1 and PC2 (Fig. 5a). In addition, PC2 is overlain by an overall coarsening-upward succession in the upper Chonan Formation that is replaced by the lower Mandano Formation with a sharp basal contact (Fig. 5a). From this stratigraphic architecture, we infer that PC1 and PC2 may have formed during an overall glacioeustatic sea-level fall from MIS 17 to MIS 16. This sea-level fall was interrupted by a short-term still-stand at MIS 16.3, which is marked by the development of a muddy interval that contains the Ch3 tephra key bed (Fig. 5b).

An abrupt glacioeustatic sea-level rise and the following fall from MIS 16.2 to MIS 15.4 formed an overall coarsening-upward succession, which is interpreted as consisting of transgressive and highstand deposits of the upper Chonan Formation and falling-stage deposits of the lower Mandano Formation in the southwestern up-slope area (Fig. 5). The sharp basal surface of the lower Mandano Formation can be assigned to a regressive surface of marine erosion (in the sense of Plint and Nummedal 2000). Because the Ch2 tephra key bed is intercalated in the uppermost part of the lower Mandano Formation and the lowest part of PC3 (Machida et al. 1980; Tokuhashi and Endo 1984) (Fig. 5a), shedding of coarse-grained sediments beyond the shelf margin may have commenced during the late falling stage, just before the uppermost part of the lower Mandano Formation was subjected to slight incision that enabled the bypassing of coarse-grained sediments to form PC3 in the northeastern downslope area. The ensuing transgression and regression are considered to have formed the marsh and shallow-marine embayment deposits of the middle Mandano Formation from MIS 15.4 to MIS

15.3 (Fig. 5b). During this period, the muddy interval that contains the Ch1 tephra key bed replaced PC3 in the northeastern downslope area (Fig. 5a).

The subsequent glacioeustatic sea-level fall from MIS 15.3 to MIS 15.2 is interpreted to have caused development of a shallow valley that represents the base of the Nagahama Formation and may have acted as a conduit to form PC4 in the northeastern down-slope area (Fig. 11b). Backfilling of the valley is considered to have occurred during the late falling and early transgressive stages, and the active supply of gravel and sand may have subsequently declined. Because the coarse-grained coastal and shallow-marine deposits of the lower Mandano Formation show an abrupt change downslope into slope deposits of the coeval Chonan Formation from locations 4 to 5 (see sections 4 and 5 in Fig. 5a), in association with a distinct clinoform that shows a downlap termination to the underlying upper Chonan Formation (Fig. S3b), the lower Mandano Formation is considered to have formed as a coarse-grained, shelf-margin delta or fan-delta system (in the sense of Porębski and Steel 2003) (Fig. 11). The clinoform and discordance in bedding within the lower section of the lower Mandano Formation (Fig. S3b–c) are interpreted to reflect progradation and switching of depocenters of the shelf-margin delta or fan delta.

PC4 was first onlapped by the outer-shelf deposits of the lower Kasamori Formation in response to the glacioeustatic sea-level rise from MIS 15.2 to MIS 15.1 (Fig. 5). Subsequently, the middle Mandano and Nagahama formations were further transgressed by the sand-ridge deposits of the upper Mandano Formation; these sand-ridge deposits were succeeded by outer-shelf muddy deposits of the middle Kasamori Formation that contains the Ks12 tephra key bed and is interpreted to comprise transgressive and highstand systems tracts (Ito 1992) (Fig. 5a).

Origins of the packets

In terms of the sequence-stratigraphic architectures of the Chonan, Mandano, and Nagahama formations, PC1–PC4 are interpreted to have formed during the falling and lowstand stages of glacioeustatic sea-level changes as a response to progradation of a coarse-grained shelf-margin delta or fan delta (Figs. 5 and 11). PU1–PU2 in the upper Umegase Formation and PK1–PK2 in the Kokumoto Formation are also interpreted to have developed in depositional and sequence-stratigraphic settings similar to those of the Chonan Formation, although their coeval coastal depositional systems are not exposed in outcrop (Figs. 3 and 4).

Depositional processes of lithofacies types in the packets

Thick- to very thick-bedded sandstones of types 1 and 2 are interpreted to have formed by the amalgamation of thinner sandstone beds as a result of either recurrent fall out of suspended loads from sustained high-density sediment gravity flows (Kneller and Branney 1995) or discontinuous fall out of suspended loads from intermittently occurring waning turbidity currents. Abrupt downflow thinning of thick- to very thick-bedded sandstones is also interpreted to be a result of *en masse* deposition from sandy debris flows (Shanmugam 1996; Talling et al. 2013a). Because type 1 and 2 sandstone beds commonly contain convolute bedding and possess erosional bases, and laterally show a transition into type 5 and 6 sandstone beds over a short distance (Fig. 10), their deposition is considered to have been induced by rapid fall out of sand particles from high-density sediment gravity flows rather than by *en masse* processes in debris flows, although flow transformation from sandy debris flows to turbulent gravity flows (in the sense of Fisher 1983) is an alternative possible process for the lateral variation in lithofacies types. Abrupt fining and thinning of thick- to very thick-bedded sandstones can alternatively be interpreted to reflect the deposition of sand particles, forming thick- to very thick-bedded sandstones that may have resulted in a decrease in the density of the residual sediment gravity flows, which initially contained lower-density fresh water and were finally transformed into buoyant flows (Gladstone and Pritchard 2010). Buoyant flows are commonly generated in hyperpycnal flows that are interpreted to be more widely occurring in river-fed turbidite systems than previously thought (Stevenson and Peakall 2010). Consequently, thick- to very thick-bedded sandstones are expected to have been deposited by hyperpycnal flows (Plink-Björklund and Steel 2004).

Sandstone beds that have single or multiple zones of inverse-to-normal grading in association with alternating parallel lamination and current-ripple cross-lamination and internal erosion surfaces (types 3 and 4) are interpreted to have formed in response to single or multiple episodes of waxing and waning of unsteady sediment gravity flows. Hyperpycnal flows (Mulder et al. 2003; Zavala et al. 2006) are possible candidate gravity flows for the development of type 3 and 4 sandstone beds. Breaching of sandy sediments in response to retrogressive failure of a sandy substrate is an alternative explanation for the initiation of single and multiple episodes of waxing and waning of sediment gravity flows (Mastbergen and Van Den Berg 2003). Because the development of the four packets (PC1–PC4) in the Chonan Formation is interpreted to have been induced by the progradation of a gravelly shelf-margin delta or fan delta, which are characterized by the development of wave-dominated

gravelly coasts, active shedding of coarse-grained sediments beyond the shelf margin is considered to have been promoted by hyperpycnal flows (Fuse et al. 2013), although collapse of delta-front sediments cannot necessarily be excluded as a possible mechanism for the origins of the component sandstone beds of the packets. Concurrent occurrence of hyperpycnal flows and collapse-induced gravity flows has been documented in the modern Sakawa River fan delta in the Sagami Bay, about 75 km west of the Boso Peninsula (location marked in the inset of Fig. 1). This fan delta underwent a large flood event in 1972, and abundant sand and gravel, together with wood and plant fragments, were transported from the river mouth into the fan-delta front and farther downslope area by gravity flows. This flood event also induced the collapse of the fan-delta slope, generating submarine landslides and gravity flows and associated submarine cable breaks (Otsuka et al. 1973). Subsequently, younger surface sediment samples were collected from this fan-delta slope; some of these sediments have been interpreted as hyperpycnites (Ikehara et al. 2018). The packets in the upper Umegase and Kokumoto formations contain lithofacies assemblages that also characterize the four packets of the Chonan Formation, and are considered to have developed via processes similar to those involved in the formation of the packets in the Chonan Formation.

In general, the sandstone beds in the packets of the three formations have a lenticular geometry, compensation stacking patterns, and laterally discontinuous distribution patterns. These architectural features suggest that the sandstone beds were formed as lenticular deposits, with limited downslope and along-slope extents, and the depressions between sand deposits, which were formed by the preceding depositional events, provided accommodation volume for the later sand deposition (Fig. 11a). Of the sandstone beds that show laterally discontinuous distribution patterns, some thinned sandstone beds can be farther correlated with thicker and coarser sandstone beds in a more downslope area (Fig. 10). These sandstone-bed distribution patterns suggest that these sandstone beds were sourced from different staging points simultaneously in association with the progradation of a shelf-margin delta or fan delta in upslope areas (Fig. 11a). In addition, PC1 and PC2 also show laterally discontinuous distribution patterns, and thicker sandstone beds are developed in a more downslope area in PC1 (Fig. 5). These distribution patterns may also indicate the development of different staging points. Consequently, the depositional setting of the packets in the three formations is interpreted to be classified as a slope apron or a ramp, characterized by a linear source system (Heller and Dickinson 1985; Stow and Johansson 2000; Stow and Mayall, 2000) that enabled coeval multiple sandbodies to develop beyond the shelf margin (Fig. 11a).

Relative timing of formation of the packets

Active delivery of coarse-grained sediments beyond the shelf-margin into deep-water environments has been considered to occur during the falling and lowstand stages of relative sea level in terms of the sequence-stratigraphic model (e.g., Posamentier and Allen 1999). Subsequently, the joint operation of several factors, including the positions of canyon heads relative to coastal and river-mouth areas, the shelf width, and the intensities of longshore currents and fluvial discharges, has been interpreted to vary the timing of the onset of active delivery of coarse-grained sediments beyond the shelf-margin into deep-water environments, particularly during the Quaternary (Covault and Graham 2010; Sweet and Blum 2016). However, these studies have focused mainly on submarine canyon–submarine fan systems, and the timing in other deep-water systems, such as slope apron and ramp systems, is not yet clearly understood. Because the packets of the upper Umegase and Kokumoto formations, as well as those of the Chonan Formation, are interpreted to have formed as slope aprons or ramps (Fig. 11), the relative timing of formation of the packets can explain some of the variation in the active delivery of coarse-grained sediments beyond the shelf-margin into deep-water environments in an active margin setting.

On the basis of the age framework of the upper Umegase and Kokumoto formations, we investigated the relative timing of the initial and final delivery of coarse-grained sediments in the development of PU1–PU2 in the upper Umegase Formation and of PK1–PK2 in the Kokumoto Formation with respect to the oxygen isotopic sea-level index as an allogenic control.

Upper Umegase Formation

The age framework of the upper Umegase Formation is based on magnetostratigraphy, oxygen isotopic stratigraphy, and nannofossil datums (Sato et al. 1988; Okada and Niitsuma 1989; Pickering et al. 1999). Except for those of Pickering et al. (1999), the age data indicate that the stratigraphic horizons containing the U4 and U3 tephra key beds can be assigned to MIS 24 and MIS 23, respectively (Kazaoka et al. 2015). PU1 and PU2 are interpreted to have formed after the abandonment of submarine-fan channel deposits and were included in the falling- and lowstand deposits of DS 11 of Ito and Katsura (1992). On the basis of the age framework described above, the packets are considered to have formed mainly during the falling and lowstand stages from MIS 23 to MIS 22 (Fig. 3). The separation of PU1 and PU2 by a muddy horizon, which contains the U2 tephra key bed (cf. Mitsunashi et al. 1959; Geological Survey of Japan 1961), is considered to have developed in response to an ephemeral lateral shift of a river mouth on the

shelf-margin delta or fan delta, or alternatively to have been induced by a minor glacioeustatic sea-level rise between MIS 23 and MIS 24 that interrupted an overall sea-level fall, as proposed by Lisiecki and Raymo (2005).

Kokumoto Formation
A detailed age framework for the Kokumoto Formation has been proposed in previous studies (Pickering et al. 1999; Kazaoka et al. 2015; Nishida et al. 2016). Tentative correlations of the bases and tops of the two packets (PK1–PK2) were made by Nishida et al. (2016) on the basis of the sequence-stratigraphic interpretation of Ito (1992) and Ito and Katsura (1992). PK1 and PK2 are considered to have been deposited between MIS 21.1 and MIS 20.2 and between MIS 18.4 and MIS 18.3, respectively (Fig. 4). Additional oxygen isotopic data from a composite section for a stratigraphic horizon between the upper part of PK1 and the lower part of PK1 (Suganuma et al. 2018) indicate that deposition of PK2 commenced during the late stage of MIS18 when the eustatic sea level fell approximately 60 m from the highest stage of MIS 19, although a minor eustatic sea-level rise occurred during this overall falling stage (Elderfield et al. 2012), similar to the ephemeral rise during MIS 18.3 reported by Bassinot et al. (1994). The minor glacioeustatic sea-level rise seems to have been documented in the formation of muddy deposits in the upper part of PK2 in location 7 in Fig. 4. The muddy deposits, which contain the Lower–Middle Pleistocene Subseries boundary, show an overall fining-upward pattern above PK1 (Fig. 4), and are interpreted to have formed close to the highest stage of eustatic sea level of Elderfield et al. (2012). This proposed boundary horizon is also considered to be in the uppermost transgressive systems tract (= downlap surface) (Fig. 4), and to have a higher potential for preserving tephra beds, although the age resolution may be limited by the development of a condensed section along the downlap surface horizon.

Variation in the relative timing of packet deposition
The timing of the initial deposition of the packets in the upper Umegase, Kokumoto, and Chonan formations varies within a single formation and between the three formations, although the packets developed mainly during the falling and lowstand stages of glacioeustatic sea-level changes. The variation is considered to have been controlled by the width of the shelf, the positions of river mouths relative to the shelf margin, the amounts of coarse-grained sediment discharges, and the magnitude and rate of falls in relative sea level.

The youngest packets of each formation were abruptly replaced by muddy deposits in the basal parts of the overlying formations, such as the basal parts of the Kokumoto, Kakinokidai, and Kasamori formations (Figs. 3, 4, and 5), although the replacement of PK2 by the basal muddy deposits of the Kakinokidai Formation occurred during the latest stage of glacioeustatic sea-level fall (Fig. 4). An abrupt reduction in the active delivery of coarse-grained sediments beyond the shelf margin may have been a response to the storage of coarse-grained sediments at river mouths on the shelf-margin deltas or fan deltas. The earlier replacement of PK2 with the muddy deposits during a late stage of glacioeustatic sea-level fall is considered to have been induced by the activation of basin subsidence, giving rise to an early commencement of relative sea-level rise before MIS18.2. Autogenic processes, such as the lateral migration of a staging point for the coarse-grained sediment supply and a short-lived decrease in the sediment discharge from the river system, may also have caused the abrupt abandonment of packet formation for PK2 and the other packets.

Conclusions
Mapping of tephra key beds within heterogeneous lithofacies assemblages can provide a detailed chronostratigraphic framework for elucidating spatial and temporal variations in depositional systems from coastal to shallow-marine and deep-water environments. This study sought to clarify (1) the origins of DWMSs in relations to coeval coastal depositional systems, and (2) the relative timing of the active delivery of coarse-grained sediments beyond the shelf margin within a chronostratigraphic framework based on the mapping of tephra key beds and oxygen isotopic data. The present case study was based on detailed outcrop investigations of (in ascending order) the upper Umegase, Kokumoto, and Chonan formations of the Pleistocene Kazusa Group on the Boso Peninsula, central Japan. The main conclusions of the study are as follows.

1. Packets of thick- to very thick-bedded sandstones, which are assigned to DWMSs, are interpreted to have developed in response to the progradation of gravelly shelf-margin deltas or fan deltas during the falling and lowstand stages of relative sea-level changes, which were controlled primarily by glacioeustasy.
2. DWMSs and associated sandstone beds generally show a lenticular geometry and compensation stacking patterns. Their lateral changes in bed thickness and grains sizes suggest that they formed in multi-sourced systems on the shelf-margin deltas or fan deltas, such as a slope apron or a ramp.
3. Initiation of sediment gravity flows, which formed DWMSs and associated sandstone beds, is considered to have been caused by hyperpycnal flows, in association with breaching and/or collapse

of coarse-grained substrates on the shelf-margin deltas or fan deltas in response to flood events.

4. The relative timing of the initial deposition and abandonment of the packets varies within and between the three studied formations. The variation is considered to have been caused by interaction between glacial and interglacial sea-level changes and basin subsidence superimposed by processes operated within the shelf-margin delta or fan-delta systems, such as the lateral migration of a staging point for the supply of coarse-grained sediment and a short-lived decrease in sediment discharge from the fluvial system.

5. Two packets are developed in the Kokumoto Formation, below and above a muddy interval that contains the Lower–Middle Pleistocene Subseries boundary (GSSP). On the basis of sequence-stratigraphic classification of these deposits, the GSSP horizon is interpreted to have formed in the uppermost part of a transgressive systems tract and can be assigned to a condensed section. This depositional setting likely promoted the development of the international type section for the Lower–Middle Pleistocene Subseries boundary in the Kazusa fore-arc basin.

Supplementary information

Supplementary information accompanies this paper at https://doi.org/10.1186/s40645-020-00343-1.

Additional file 1: Figure S1. Sequence-stratigraphic classification and spatial and temporal variations in depositional systems of the Kazusa Group on the Boso Peninsula, central Japan. Modified from Ito and Katsura (1992) and Ito et al. (2016). The red arrow on the right side of section 13 indicates the stratigraphic position of the Chiba composite section. The inset map shows the locations of the measured sections.

Additional file 2: Figure S2. Outcrop photographs of the Chonan Formation. **a** Muddy deposits containing the Ch1 tephra key bed, underlain and overlain by PC3 and PC4, respectively (Oto, Ichihara City). **b** Very thick-bedded sandstone bed occurring just below the Ch2 tephra key bed and containing convolute bedding and minor normal grading in the uppermost part (Itabu, Ichihara City). **c** Normally graded, medium- to very fine-grained sandstones and graded siltstones containing abundant plant fragments (Koshikiya, Ichihara City). **d** Inversely and normally graded sandstone bed with current-ripple cross-lamination and parallel lamination in PC3 (Heizo, Ichihara City). **e** Alternation of current-ripple cross-lamination and parallel-lamination within a sandstone bed that also contains massive and normally graded bedding and an internal erosion surface (Koshikiya, Ichihara City). **f** Ungraded, very thin- to thin-bedded, medium- to fine-grained sandstone beds (arrowed) (Koshikiya, Ichihara City). **g** Hummocky cross-stratified, fine-grained sandstone bed (Kururioyatsu, Kimitsu City). **h** Unconformable contact between the Ichijiku and Chonan formations (Okuradai, Kimitsu City).

Additional file 3: Figure S3. Outcrop photographs of the Mandano Formation. **a** Sharp basal contact between the Chonan and lower Mandano formations (Minowa, Kimitsu City). **b** Distinct clinoform in the lower part of the Mandano Formation (Mandano, Ichihara City). **c** Scour and bedding discordance in the lower section of the lower Mandano Formation (Minowa, Kimitsu City). **c** Medium- to very coarse-grained sandstones and intercalated pebble-sized conglomerates in the middle

---

section of the lower Mandano Formation (Minowa, Kimitsu City). Trough cross-stratified conglomerates rest on a sharp contact.

Additional file 4: Figure S4. a Lithofacies succession from the lower to the middle and upper parts of the Mandano Formation (Yoshino, Kimitsu City). The basal parts of the middle and upper Mandano Formation show slightly erosional contacts. Ch1 and Ch2 are tephra key beds that are also intercalated in the Chonan Formation (see a and b in Fig S2). **b** Block sample of muddy deposits of the middle Mandano Formation containing shallow-marine molluscan shells (Minowa, Kimitsu City). **c** Lithofacies succession from the lower to upper parts of the Mandano Formation (Yoshino, Kimitsu City). Muddy deposits of the middle Mandano Formation were removed by the erosional base of the upper Mandano Formation that is characterized by trough cross-stratification and shows an overall fining-upward pattern. **d** Shallow-marine molluscan fossils intercalated in trough cross-stratified medium- to very coarse-grained sandstones of the upper Mandano Formation (Yoshino, Kimitsu City).

Additional file 5: Figure S5. Outcrop photographs of the Nagahama Formation. **a** Gently undulating waveforms and foreset bedding in conglomerates and overlying pebbly sandstones in the basal part of the Nagahama Formation (Tsukuriki, Kimitsu City). Solid and dotted red lines indicates an unconformable contact. **b** Trough cross-bedded conglomerates in the basal part of the Nagahama Formation (Sasage, Futtsu City). The solid red line indicates an unconformable contact. **c** Lithofacies succession from the Ichijiku to the Nagahama and the upper Mandano formations (Manobori, Kimitsu City). A person is circled for scale.

Additional file 6: Figure S6. Outcrop photographs of the lithofacies types summarized in Table 1. Solid white and black arrows indicate the base and top of each sandstone bed, respectively. **a** Very thick-bedded, ungraded and convoluted, medium-grained sandstone bed of the Umegase Formation (Type 1). **b** Very thick-bedded, ungraded and convoluted sandstone bed, with minor normal grading in the uppermost 10 cm of the Umegase Formation (Type 2). **c** Climbing-ripple-laminated, fine- to very fine-grained sandstone bed with inverse and normal grading of the Kokumoto Formation (Type 3). **d** Type 4 sandstone bed with alternating parallel laminations and current-ripple cross-laminations of the Kokumoto Formation. **e** Medium-bedded, ungraded, medium- to fine-grained sandstone bed of the Umegase Formation (Type 5). **f** Normally graded sandstone bed with parallel laminations with lignite (L) and current-ripple cross-laminations in the uppermost 3 cm of the Umegase Formation (Type 6).

Availability of data and materials

Please contact the corresponding author for data request.

Author details

[1]Mitsubishi Corporation, 2-3-1 Marunouchi, Chiyoda-ku, Tokyo 100-8086, Japan. [2]JX Nippon Oil & Gas Exploration Co., Ltd., 1-1-2 Otemachi, Chiyoda-ku, Tokyo 100-8163, Japan. [3]Mitsui Oil Exploration Co., Ltd., 1-2-9

Nishi Shimbashi, Minato-ku, Tokyo 105-0003, Japan. [4]Chiba Prefecture, 1-1-1 Ichiba-cho, Chiba 260-8667, Japan. [5]Godo Shigen, Co. Ltd., 1365 Nanaido, Chiba 299-4333, Japan. [6]Japan Oil, Gas and Metals National Corporation, 2-10-1 Toranomon, Minato-ku, Tokyo 105-0001, Japan. [7]Department of Environmental Sciences, Tokyo Gakugei University, 4-1-1 Nukuikita, Tokyo 184-8501, Japan. [8]Department of Earth Sciences, Chiba University, Chiba 263-8522, Japan.

References

Ahokas JM, Nystuen JP, Martinius AW (2014) Stratigraphic signatures of punctuated rise in relative sea-level in an estuary-dominated heterolithic succession: incised valley fills of the Toarcian Ostrealv Formation, Neill Klinter Group (Jameson land, East Greenland). Mar Petrol Geol 50:103–129

Allen JRL (1997) Simulation models of salt-marsh morphodynamics: some implications for high-intertidal sediment couplets relate to sea-level change. Sediment Geol 113:211–223

Baba K (1990) Molluscan fossil assemblages of the Kazusa Group, southern Kwanto, Central Japan. Keiyo Yochisha, Tokyo

Bartholdy J, Brivio L, Bartholdy A, Kim D, Fruergaard M (2017) The Skallingen spit. Denmark: birth of a back-barrier saltmarsh Geo-Mar Lett doi. https://doi.org/10.1007/s00367-017-0523-5

Bassinot FC, Labeyrie LD, Vincent E, Quidelleur X, Shackleton NJ, Lancelot Y (1994) The astronomical theory of climate and the age of the Brunhes–Matuyama magnetic reversal. Earth Planet Sci Lett 126:91–108

Bluck BJ (2011) Structure of gravel beaches and their relationship to tidal range. Sedimentology 58:994–1006

Blum M, Rodgers K, Gleason J, Najman Y, Cruz J, Fox L (2018) Allogenic and autogenic signals in the stratigraphic record of the deep-sea Bengal fan. Sci Rep 8(7973):1–13

Bouma AH (1962) Sedimentology of some flysch deposits: a graphical approach to facies interpretation. Elsevier, Amsterdam

Boyd R, Dalrymple RW, Zaitlin BA (2006) Estuarine and incised-valley facies models. In: Posamentier HW, Walker RG (eds) Facies models revisited. SEPM Spec Publ 84:171–235

Burningham H (2015) Gravel spit-inlet dynamics: Oxford spit, UK. In: Randazzo G, Jackson DWT, Cooper JAG (eds) Sand and gravel spits. Springer, Cham

Campbell SE (1967) Lamina, laminaset, bed and bedset. Sedimentology 8:7–26

Clifton HE (2006) A reexamination of facies models for clastic shorelines. In: Posamentier HW, Walker RG (eds) Facies models revisited. SEPM Spec Publ 84:293–337

Covault JA, Graham SA (2010) Submarine fans at all sea-level stands: Tectonomorphic and climatic controls on terrigenous sediment delivery to the deep sea. Geology 38:939–942

Davidson-Arnott R (2010) Introduction to coastal processes and geomorphology. Cambridge Univ Press, Cambridge

Dumas S, Arnott RWC, Southard JB (2005) Experiments on oscillatory-flow and combined-flow bed forms: implication for interpreting parts of shallow-marine sedimentary record. J Sediment Res 75:501–513

Elderfield H, Ferretti P, Greaves M, Crowhurst S, McCave IN, Hodell D, Piotrowski AM (2012) Evolution of ocean temperature and ice volume through the mid-Pleistocene climate transition. Science 337:704–709

Fisher RV (1983) Flow transformation of sediment gravity flows. Geology 11:273–274

Fuse M, Nakamura K, Ito M (2013) Geometry and internal organization of hyperpycnites formed in front of a shelf-margin delta system, a middle Pleistocene Chonan Formation on the Boso Peninsula, Central Japan. J. Sediment Soc Japan 72:147–151

Galy V, France-Lanord C, Beysssac O, Faure P, Kudras H, Palhol F (2007) Efficient organic carbon burial in the Bengal fan sustained by the Himalayan erosional system. Nature 450:407–410

Geological Survey of Japan (1961) Geological maps of the oil and gas field of Japan 4 Futtsu–Otaki

Gladstone C, Pritchard D (2010) Patterns of deposition from experimental turbidity currents with reversing buoyancy. Sedimentology 57:53–84

Hart BS, Plint AG (1989) Gravelly shoreface deposits: a comparison of modern and ancient facies sequences. Sedimentology 36:551–557

Heller PL, Dickinson WR (1985) Submarine ramp facies model for delta fed, sand-rich turbidite systems. Am Ass Petrol Geol Bull 69:960–976

Hirayama J, Nakajima T (1977) Analytical study of turbidites, Otadai Formation, Boso Peninsula, Japan. Sedimentology 24:747–779

Hiroki Y, Masuda F (2000) Gravelly spit deposits in a transgressive systems tract: the Pleistocene Higashikanbe gravel, Central Japan. Sedimentology 47:135–149

Hodgson, D.M, Bernhard A, Clare MA, Da Silva A-C, Fosdick JC, Mauz B, Midtkandal I, Owen A, Romans BR (2018) Grand challenges (and great opportunities) in sedimentology, stratigraphy, and diagenesis research. Fron. Earth Sci. 6/173:1–9

Ikehara K, Sugisaki S, Ajioka T, Katayama H (2018) Sedimentological evidences on storm-induced density bottom currents on the Sakawa fan-delta slope, Japan. AGU fall meeting abstract OS13C-1501

International Commission on Stratigraphy (2020) International chronostratigraphic chart. http://www.stratigraphy.org/index.php/ics-chart-timescale

Ito H, Nanayama F, Nakazato H (2017) Zircon U–Pb dating using LS-ICP-MS: quaternary tephras in Boso Peninsula, Japan. Quat Geochronol 40:12–22

Ito M (1992) High-frequency depositional sequences of the upper part of the Kazusa Group, a middle Pleistocene forearc basin fill in Boso Peninsula, Japan. Sediment Geol 76:155–175

Ito M (1995) Volcanic ash layers facilitate high-resolution sequence stratigraphy at convergent plate margins: an example from the Plio–Pleistocene forearc basin fill in the Boso Peninsula, Japan. Sediment Geol 95:187–206

Ito M (1998) Contemporaneity of component units of the lowstand systems tract: an example from the Pleistocene Kazusa forearc basin, Boso Peninsula, Japan. Geology 26:939–942

Ito M (2019) Lithofacies architecture of gravel-wave deposits: insight into the origins of coarse-grained gravity-flow deposits. Sediment Geol 382:36–46

Ito M, Ishimoto S, Ito K, Kotake N (2016) Geometry and lithofacies of coarse-grained injectites and extrudites in a late Pliocene trench-slope basin on the southern Boso Peninsula, Japan. Sediment Geol 344:336–349

Ito M, Katsura Y (1992) Inferred glacio-eustatic control for high-frequency depositional sequences of the Plio–Pleistocene Kazusa Group, a forearc basin fill in Boso Peninsula, Japan. Sediment Geol 80:67–75

Ito M, Masuda F (1988) Late Cenozoic deep-sea to fan-delta sedimentation in an arc–arc collision zone, Central Honshu, Japan: sedimentary response to varying plate tectonic regime. In: Nemec W, Steel RJ (eds) Fan deltas: sedimentology and tectonic settings. Blackie, Glasgow and London

Ito M, Nishida N, Otake S, Saito T, Okazaki H, Nishikawa T (2006a) Glacioeustatic signals and sequence architecture of the Pliocene–Pleistocene forearc basin-fill successions on the Boso Peninsula, central Japan. In: Ito M, Yagishita K, Ikehara K, Matsuda H (eds) Field excursion guidebook, 17th international sedimentological congress, Fukuoka, Japan. Sediment Soc Japan FE-A4:1–30

Ito M, Saito T (2006) Gravel waves in an ancient canyon: analogous features and formative processes of coarse-grained bedforms in a submarine-fan system, the lower Pleistocene of the Boso Peninsula, Japan. J. Sediment Res 76:1274–1283

Ito M, Takao A, Ishikawa K, Himeno O (2006b) A new venue of sedimentological study of deep-water successions: reorganization of the lowstand depositional model. J Japan Ass Petrol Tech 71:21–33

Kazaoka O, Suganuma Y, Okada M, Kameo K, Head M, Yoshida T, Sugaya M, Kameyama S, Ogitsu I, Nirei H, Aida N, Kumai H (2015) Stratigraphy of the Kazusa Group, Boso Peninsula: an expanded and highly-resolved marine sedimentary record from the Lower and Middle Pleistocene of Central Japan. Quat Int 383:116–135

Kitazato H (1997) Paleogeographic changes in Central Honshu, Japan, during the late Cenozoic in relation to the collision of the Izu–Ogasawara arc with the Honshu arc. Island Arc 6:144–157

Kneller BC (1995) Beyond the turbidite paradigm: physical models for deposition of turbidites and their implications for reservoir prediction. In: Hartley AJ, Prosser DJ (eds) Characterization of deep marine clastic systems. Geol Soc. London 94:31–49.

Kneller BC, Branney MJ (1995) Sustained high-density turbidity currents and the deposition of thick massive sands. Sedimentology 42:607–616

Lisiecki LE, Raymo ME (2005) A Pliocene–Pleistocene stack of 57 globally distributed benthic $\delta^{18}O$ records. Paleoceanography 20:PA1003. https://doi.org/10.1029/2004PA001071

Lowe DR (1982) Sediment gravity flows: II. Depositional models with special reference to the deposits of high-density turbidity currents. J Sediment Res 52:279–297

Machida H, Arai F (2011) Atlas of tephra in and round Japan. Tokyo Univ Press, Tokyo

Machida H, Arai F, Sugihara S (1980) Tephrochronological study on the middle Pleistocene deposits in the Kanto and Kinki districts, Japan. Quat Res 19:233–261

Massari F, Parea GC (1988) Progradational gravel bed sequences in a moderate-to-high energy, microtidal environment. Sedimentology 35:881–913

Mastbergen DR, Van Den Berg JH (2003) Breaching in fine sands and the generation of sustained turbidity currents in submarine canyons. Sedimentology 50:625–637

Mitsunashi T (1990) Synsedimentary tectonics of the southern part of the Kanto sedimentary basin, Central Japan. Mem Geol Soc Japan 34:1–9

Mitsunashi T, Yasukuni N, Shinada Y (1959) Stratigraphical section of the Kazusa Group along the shores of the rivers Yoro and Obitsu. Bull Geol Surv Japan 10:9–24

Morsilli M, Pomar L (2012) Internal waves vs. surface storm waves: a review on the origin of hummocky cross-stratification. Terra Nova 24:273–282

Mulder T, Alexander J (2001) Physical character of subaqueous sedimentary density currents and their deposits. Sedimentology 48:269–299

Mulder T, Syvitski JPM, Migeon S, Faugéres J-C, Savoye B (2003) Hyperpycnal turbidity currents: initiation, behavior and related deposits: a review. J Mar Petrol Geol 20:861–882

Nakajima J, Hasegawa A (2010) Cause of M~7 intraslab earthquakes beneath the Tokyo metropolitan area, Japan: possible evidence for a vertical tear at the easternmost portion of the Philippine Sea slab. J Geophys Res 115(B04301):1–16

Nakajima T, Watanabe M (2005) Geology of the Futtsu district. Quadrangle Ser. 1: 50,000. Geol. Surv. Japan, AIST, Ibaraki

Nanayama F, Nakazato H, Ooi S, Nakashima R (2016) Geology of the Mobara district. Quadrangle Ser. 1 : 50,000, Geol Surv Japan, AIST

Nielsen LH, Johannessen PN (2008) Are some isolated shelf sandstone ridges in the cretaceous Western interior seaway transgressed, detached spit systems? SEPM Spec Publ 90:333–354

Nishida N, Ajioka T, Ikehara K, Nakashima R, Utsunomiya M (2019) Spatial variation and stratigraphy of the marine sediments off the east coast of the Boso Peninsula, Pacific Ocean, Japan. Seamless geoinformation of coastal zone "Eastern coastal zone of Boso Peninsula". Geol Surv Japan

Nishida N, Kazaoka O, Izumi K, Suganuma Y, Okada M, Yoshida T, Ogitsu I, Nakazato H, Kameyama S, Kagawa A, Morisaki M, Nirei H (2016) Sedimentary processes and depositional environments of a continuous marine succession across the lower–middle Pleistocene boundary: Kokumoto Formation, Kazusa Group, Central Japan. Quat Int 397:3–15

Okada M, Niitsuma N (1989) Detailed paleomagnetic records during the Brunhes–Matuyama geomagnetic reversal, and a direct determination of depth lag for magnetization in marine sediments. Phys Earth Planet Inter 56:133–150

Otsuka K, Kagami H, Honza E, Nasu N, Kobayashi K (1973) Submarine slumping as a cause of turbidity currents in Sagami Bay. Mar Sci 446:14–20

Peters SE, Loss DP (2012) Storm and fair-weather wave base: a relevant distinction? Geology 40:511–514

Pickering KT, Souter C, Oba T, Taira A, Schaaf M, Platzman E (1999) Glacio-eustatic control on deep-marine clastic forearc sedimentation, Pliocene–mid-Pleistocene (*c.* 1180–600 ka) Kazusa Group, SE Japan. J Geol Soc Lond 156:125–136

Plink-Björklund P, Steel RJ (2004) Initiation of turbidity currents: outcrop evidence for Eocene hyperpycnal flow turbidites. Sediment Geol 165:29–52

Plint AG, Nummedal D (2000) The falling stage systems tract: recognition and importance in sequence stratigraphic analysis. In: hunt D, Gawthorpe RL (eds) sedimentary response to forced regressions. Geol Soc Spec Publ 172:1–17

Porębski SJ, Steel RJ (2003) Shelf-margin deltas: their stratigraphic significance and relation to Deepwater sands. Earth-Sci Rev 62:283–326

Posamentier HW, Allen G.P (1999) Siliciclastic sequence stratigraphy–concepts and applications. SEPM Concepts in Sedimentology and Paleontology #7

Quin JG (2011) Is most hummocky cross-stratification formed by large-scale ripples? Sedimentology 58:1414–1433

Sakai T, Masuda F (1996) Sequence stratigraphy of the upper part of the Plio–Pleistocene Kakegawa Group, western Shizuoka, Japan. J Sediment Res 66:778–787

Sato T, Takayama T, Kato M, Kudo T, Kameo K (1988) Calcareous microfossil biostratigraphy of the uppermost Cenozoic formations distributed in the coast of the Japan Sea, part 4: conclusion. J Japan Ass Petrol Technol 53:474–491

Satoguchi Y (1995) Tephrostratigraphy in the lower and middle Kazusa Group in the Boso Peninsula, Japan. J Geol Soc Japan 101:767–782

Shanmugam G (1996) High-density turbidity currents: are they sandy debris flow? J Sediment Res 66:2–10

Shirai M (2001) Middle Pleistocene widespread tephras found in the eastern Japan Sea. Earth Monthly 23:600–604

Stevenson CJ, Peakall J (2010) Effects of topography on lofting gravity flows: implications for the deposition of deep-water massive sands. Mar Petrol Geol 27:1366–1378

Stow DAV, Johansson M (2000) Deep-water massive sands: nature, origin, and hydrocarbon implications. Mar Petrol Geol 17:145–174

Stow DAV, Mayall M (2000) Deep-water sedimentary systems: new models for the 21st century. Mar Petrol Geol 17:125–135

Stow DAV, Shanmugam G (1980) Sequence of structures in fine-grained turbidites: comparison of recent deep-sea and ancient flysch sediments. Sediment Geol 25:23–34

Suganuma Y, Haneda Y, Kameo K, Kubota Y, Hayashi H, Itaki T, Okada M, Head MJ, Sugaya M, Nakazato H, Igarashi A, Shikoku K, Hongo M, Watanabe M, Satoguchi Y, Takeshita Y, Nishida N, Izumi K, Kawamura K, Kawamata M, Okuno J, Yoshdia T, Ogitsu I, Yabusuki H, Okada M (2018) Paleoclimatic and paleoceanographic records through marine isotope stage 19 at the Chiba composite section, Central Japan: key reference for the Early–Middle Pleistocene subseries boundary. Quat Sci Rev 19:406–430

Sweet ML, Blum MD (2016) Connections between fluvial to shallow marine environments and submarine canyons: implications for sediment transfer to deep water. J Sediment Res 86:1147–1162

Swift DJP, Parson BS, Foyle A, Oertel GF (2003) Between beds and sequences: stratigraphic organization at intermediate scales in the quaternary of the Virginia coast, USA. Sedimentology 50:81–111

Talling PJ, Malgesini G, Felletti F (2013a) Can liquefied debris flows deposit clean sand over large areas of sea floor? Field evidence from the Marnoso-arenacea formation, Italian Apennines. Sedimentology 60:720–762

Talling PJ, Masson DG, Sumner EJ, Malgesini G (2012) Subaqueous sediment density flows: depositional processes and deposits types. Sedimentology 59:1937–2003

Talling PJ, Paull CK, Piper DJW (2013b) How are subaqueous sediment density flows triggered, what is their internal structure and how does it evolve? Direct observation from monitoring of active flows. Earth Sci Rev 125:244287

Tamura I, Mizuno K, Utsunomiya M, Nakajima T, Yamazaki H (2019) Widespread tephras of the Kazusa Group distributed in the Boso Peninsula, Chiba Prefecture, Japan: especially, tephrostratigraphy and terphra correlation of the lower part of the Kazusa group. J Geol Soc Japan 125:23–39

Tokuhashi S, Endo H (1984) Geology of the Anesaki district. Quadrangle Ser. 1: 50,000. Geol Surv Japan

Zavala C, Ponce J, Drittaniti D, Arcuri M, Freije H, Asensio M (2006) Ancient lacustrine hyperpycnite: a depositional mode; from a case study in the Rayoso Formation (Cretaceous) of west-central Argentina. J Sediment Res 76:41–59

Publisher's Note